

AD-A100 210

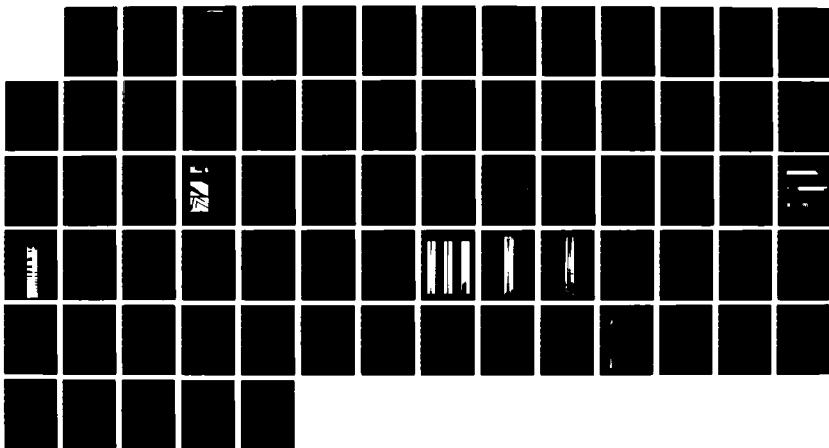
INTENSE XUV (EXTREME ULTRAVIOLET) RADIATION SOURCES(U)  
MARYLAND UNIV COLLEGE PARK INST FOR PHYSICAL SCIENCE  
AND TECHNOLOGY M L GINTER 31 JUL 85 AFOSR-TR-87-0295  
F49620-83-C-0130

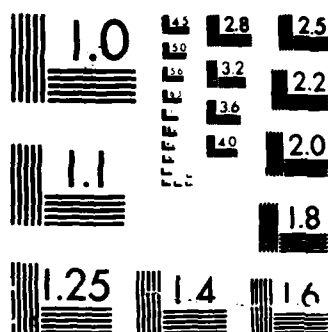
1/1

UNCLASSIFIED

F/G 20/6

NL





MICROCOPY RESOLUTION TEST CHART  
NATIONAL BUREAU OF STANDARDS 1963-A

# DTIC FILE COPY

UNCLASSIFIED

SECURITY CLASSIFICATION OF THIS PAGE

## REPORT DOCUMENTATION PAGE

1a. REPORT SECURITY CLASSIFICATION Unclassified		1b. RESTRICTIVE MARKINGS	
AD-A180 218		3. DISTRIBUTION/AVAILABILITY STATEMENT Approved for public release; distribution unlimited.	
		5. MONITORING ORGANIZATION REPORT NUMBER(S) AFOSR-TR- 87-0296	
6a. NAME OF PERFORMING ORGANIZATION Univ of Maryland	6b. OFFICE SYMBOL (If applicable)	7a. NAME OF MONITORING ORGANIZATION AFOSR	
6c. ADDRESS (City, State and ZIP Code) Institute for Physical Science & Technology College Park Maryland 20742		7b. ADDRESS (City, State and ZIP Code) Bldg 410 Bolling AFB, D.C. 20332-6448	
8a. NAME OF FUNDING/SPONSORING ORGANIZATION AFOSR	8b. OFFICE SYMBOL (If applicable) NP	9. PROCUREMENT INSTRUMENT IDENTIFICATION NUMBER F49620-83-C-0130	
8c. ADDRESS (City, State and ZIP Code) same as 7b.		10. SOURCE OF FUNDING NOS.	
		PROGRAM ELEMENT NO. 6 1102F	TASK NO. 2301
		WORK UNIT NO. A1	
11. TITLE (Include Security Classification) "INTENSE XUV RADIATION SOURCES" (U)			
12. PERSONAL AUTHOR(S) Dr. Ginter			
13a. TYPE OF REPORT ANNUAL/FINAL	13b. TIME COVERED FROM Aug 83 TO 31 Jul 85	14. DATE OF REPORT (Yr., Mo., Day)	15. PAGE COUNT 71
16. SUPPLEMENTARY NOTATION			
17. COSATI CODES		18. SUBJECT TERMS (Continue on reverse if necessary and identify by block number)	
FIELD	GROUP	SUB. GR.	
		Radiation, XUV	
19. ABSTRACT (Continue on reverse if necessary and identify by block number)			
<p>In the research characterizations were performed of the XUV output of our laser produced plasma system in the 30-1200 A region and have used the system for ptrliminary studies in high resolution spectroscopy in the grazing incidence region and in soft x-ray microlithography.</p>			
20. DISTRIBUTION/AVAILABILITY OF ABSTRACT UNCLASSIFIED/UNLIMITED <input type="checkbox"/> SAME AS RPT <input checked="" type="checkbox"/> DTIC USERS <input checked="" type="checkbox"/>		21. ABSTRACT SECURITY CLASSIFICATION UNCLASSIFIED	
22a. NAME OF RESPONSIBLE INDIVIDUAL DR. HOWARD R. SCHLOSSBERG		22b. TELEPHONE NUMBER (Include Area Code) (202) 767-4906	22c. OFFICE SYMBOL NP

MAY 11 1987

INTENSE XUV RADIATION SOURCES

Sponsored by the  
Air Force Office of Scientific Research  
under  
Contract F49620-83-C-0130

AFOSR-TR- 87-0295

ABSTRACT

We have performed characterizations of the XUV output of our laser produced plasma system in the 30-1200 Å region and have used the system for preliminary studies in high resolution spectroscopy in the grazing incidence region and in soft x-ray microlithography.

TABLE OF CONTENTS:

Technical Summary . . . . .	1
Appendix A: Laser Produced Plasma Light Sources . . . . .	3
Appendix B: XUV and Soft X-ray Radiation from Laser Produced . . . . .	23
Plasmas as Laboratory Spectroscopic Sources . . . . .	
Appendix C: Laser Produced Plasma Light Sources for High Resolution . . . . .	24
XUV and VUV Spectroscopy . . . . .	
Appendix D: Soft X-ray Lithography Using Radiation From Laser . . . . .	25
Produced Plasmas . . . . .	
Appendix E: Laser Produced Plasma Light Sources for High . . . . .	29
Resolution XUV and VUV Spectroscopy . . . . .	
Appendix F: High Resolution Spectra of Laser Plasma Light . . . . .	39
Sources in the Grazing Incidence Region . . . . .	
Appendix G: Photometric Investigation of a Laser Produced . . . . .	48
Plasma VUV Light Source . . . . .	

Approved for public release;  
distribution unlimited.

AIR FORCE OFFICE OF SCIENTIFIC RESEARCH (AFOSR)  
NOTICE OF TRANSMITTAL RIGHTS  
THIS DOCUMENT CONTAINS INFORMATION THAT IS  
PROPERTY OF THE AIR FORCE OFFICE OF SCIENTIFIC RESEARCH AND IS  
NOT TO BE DISTRIBUTED OUTSIDE THE AIR FORCE OFFICE OF SCIENTIFIC RESEARCH  
WITHOUT THE WRITTEN PERMISSION OF THE INFORMATION DIVISION



87 5 1 030

## TECHNICAL SUMMARY

This section will be restricted to a brief summary of the major technical advances made under this contract since its inception. Detailed discussions of several portions of these efforts can be found in Appendices A through G. Results have been presented at four meetings which are listed\* on the title pages of Appendices A through C, three completed scientific papers which appear in Appendices D through F, and a scientific paper in preliminary draft (Appendix G).

Radiation from laser produced plasmas has been shown to be an efficient source in both extreme ultraviolet (EUV) and soft x-ray regions of the spectrum and can be used to produce XUV outputs in the 10-300eV region with efficiencies <5%. Laser plasma light sources have been reviewed, their properties summarized, and their outputs compared with synchrotron radiation (Appendix A). Appendices A and D also place the 10 Hz repetition rate light source currently utilized in our research in perspective in the field of XUV radiation sources used for lithography, spectroscopy, and other EUV and XUV applications.

We have performed a number of studies of soft x-ray lithography using radiation from our laser plasma source. In this source, plasmas are formed by focusing ~0.6J pulses from 10 Hz Nd:YAG laser onto solid targets, and the resulting radiation is used to expose masked photoresist coated silicon wafers. Results using steel, copper, and tungsten targets show (a) that  $\text{Fe} > \text{Cu} > \text{W}$  is the order of greatest efficiency of photoresist exposure, (b) that the rates (i.e., depth per unit time which we evaluated in our experiments) of exposure of several photoresists by these targets are ~5-10 $\times$  lower than the NSLS synchrotron and (c) that laser plasma exposures of ~1-2 sq. inches are much more uniformly exposed than exposures made using the VUV storage ring at NSLS (see Appendix D for additional details).

We have performed a number of studies of the XUV spectra obtained from our laser produced plasmas using the highest spectral resolution spectrograph currently available for the ~30-400 Å region - the 10.7-m grazing incidence spectrograph at NBS (Gaithersburg, MD). We find (a) that at the highest

---

\*The fourth paper "Inner Shell Electron Excitation in Free Atoms and Atoms in Solids" was presented at the Symposium on the Application of X-Ray Lasers at Pacific Grove, California, Feb. 17-20, 1985.

available resolution the radiation from a Yb plasma target driven with  $10^{10} - 10^{11} \text{ W cm}^{-2}$  of  $1.064 \mu$  radiation produces an essentially line-free continuum between  $\sim 35$  and  $525 \text{ \AA}$ , (b) that the tungsten continuum has spectral regions where absorption lines (which are W target specific) present some problems to certain kinds of experiments, and (c) that the Cu many-line plus continuum spectrum is mostly lines over a weaker continuum except below  $\sim 60 \text{ \AA}$  where careful focusing of the plasma spot can remove most of the line spectra (see Appendices E and F for additional details).

We have performed a number of studies of EUV spectra obtained from our laser produced plasmas using the highest spectral resolution spectrograph currently available for the  $\sim 400 - 1200 \text{ \AA}$  region - the 6.65-m normal incident spectrograph at the Univ. of MD. equipped with 4800  $\ell/\text{mm}$  gratings. Under conditions similar to those outlined in the preceding paragraph we found similar results to those outlined above and have used the source to obtain examples of very highly resolved absorption and emission spectra in the EUV region (see Appendix E for further detail).

In order to allow a comparison of the intensity of different target materials as a function of wavelength, we have studied laser produced plasmas with a 1-m grazing incidence spectrograph and a multichannel photoelectric detector at NBS. The Nd:YAG laser and our basic target configuration ( $10^{11} \text{ W cm}^{-2}$ ) were used with W, Sm, Hf, Sn, Pb, Cu and steel targets with several samples on a single rotating shaft to allow comparison of different sources at each wavelength without breaking vacuum or changing the optical configuration. The observations are made between  $85 \text{ \AA}$  and  $405 \text{ \AA}$  and the variation between clean continua (Yb), good continua with absorption lines (W) or emission lines (Hf, Sm), and weaker continua with strong emission lines are observed. Work is still underway but comparisons of relative intensities at  $170 \text{ \AA}$  ( $\text{W} > \text{Hf} \approx \text{steel} > \text{Pb} > \text{Sm} \approx \text{Sn}$ ) and  $315 \text{ \AA}$  ( $\text{Sm} > \text{Hf} > \text{Pb} > \text{W} > \text{steel} > \text{Sn}$ ) have been obtained. A preliminary report on this work appears in Appendix G.

APPENDIX A

LASER PRODUCED PLASMA LIGHT SOURCES

Thomas J. McIlrath  
Institute for Physical Science and Technology  
University of Maryland  
College Park, Maryland 20742

Workshop on VUV and X-Ray Sources  
Committee on Atomic and Molecular Science  
Washington, D.C.  
Nov. 9, 1984

## Abstract

Radiation from laser produced plasmas has been shown to be an efficient source in both the extreme ultraviolet (XUV) and soft x-ray region of the spectrum. The XUV radiation can be produced as a clean continuum between 10ev and 300ev with efficiencies  $>5\%$ . Generation of x-rays as a mixture of lines and continua can be achieved with  $\approx 10\%$  efficiency for generation of .7-20 kev radiation. Laser produced plasma sources complement synchrotron radiation sources in that they have high peak fluxes but lower average intensities. Laser plasma sources can be run in a variety of environments and in many cases provide a modest cost, portable source of highly controllable and reproducible radiation.



## Introduction:

Hot plasmas have been the major laboratory source of intense radiation in the visible and ultraviolet throughout the period characterized as modern physics. This is especially true for radiation in the extreme ultraviolet (XUV) below 100nm where the blackbody temperature necessary to produce appreciable radiation exceeds the boiling point of the most refractory materials. The traditional approach has been to either run a discharge in a gas or to strike an arc between two electrodes so that the discharge runs through the vaporized material. In either case a plasma with a high electron temperature (1-20ev) can be obtained. The electrical plasma discharges are well treated in Sampson's book on Vacuum Ultraviolet Spectroscopy<sup>1</sup>. In recent years synchrotron radiation light sources have played a major role in extreme ultraviolet physics. However, these sources exist as facilities rather than traditional laboratory light sources. Furthermore, they complement rather than compete with plasma sources in that they are continuous sources of high average brightness while plasma sources at short wavelengths are pulsed with high peak brightness.

Electrical discharge plasmas are limited in the amount of energy which can be deposited in a small volume in a minimum time which limits the maximum temperature in the plasma. It was realized very early that the extremely high brightness of pulsed lasers provides an ideal mechanism for heating plasma sources. Ehler and Weissler<sup>2</sup> used a Q-switched ruby laser of 100MW peak power to study the VUV radiation from various target materials. Since that time the spectral region of study has been extended into the x-ray regime while the powers available have been raised several orders of magnitude. The aim of this paper is to give a brief, but by no means exhaustive, summary of the status of laser plasmas as extreme ultraviolet (XUV) and x-ray light sources.

## Nature of Laser Plasma Sources

Laser produced plasmas light sources are generally solid targets that are vaporized and heated by intense, short duration, focused laser beams. Liquid Hg has also been used to provide self healing, long lived targets<sup>3</sup>. Incident power densities vary from  $10^{11} \text{ Wcm}^{-2}$  to  $10^{16} \text{ Wcm}^{-2}$  and the dense plasma is heated by inverse bremsstrahlung and radiates by bremsstrahlung, recombination and line emission. The sources themselves are simple metal rods or foils and the size, expense and portability of the system are determined by the properties of the lasers. For XUV radiation the laser can be a Nd:YAG system of modest cost and sufficiently portable to be carried from laboratory to laboratory as the need arises. For the most intense x-ray sources large kilojoule lasers in fixed facilities are used. Intermediate sized systems such as slab glass or excimer lasers should provide sources of x-rays to  $\geq 2$  keV at a cost and complexity which is appropriate for small laboratories as opposed to facilities.

The radiation from laser produced plasmas varies from very pure continuum emission to predominantly line sources depending on the choice of target material and the spectral region of study. The plasmas are very high intensity, pulsed sources of low duty cycle with a pulse duration determined by the driving laser down to  $\leq 10^{-10}$  sec duration. The radiation is unpolarized and nearly isotropic and is highly reproducible. Although the radiant power produced is comparable to that produced by synchrotron radiation sources, the very different output parameters make comparisons of the sources difficult and the two sources in fact are complementary rather than directly competitive.

One particularly useful feature of laser plasma sources is the absence of any requirement for high vacuum conditions. Sources are easily run with an atmosphere of 100 torr of background gas or more with no apparent effect

on the emission. Thus He can be introduced into the source chamber to absorb much of the XUV radiation while transmitting the soft x-ray output<sup>3,4</sup>. Similarly, laser plasma sources have been inserted into atomic vapors and used in situ as sources of ionizing radiation for pumping metastable ionic systems<sup>5</sup>. In general, the sources are compatible with most conditions which are consistent with the use of XUV or x-ray radiation.

#### Sources of Radiation. $\leq 300\text{ev}$ ( $\geq 4\text{nm}$ )

Intense sources of radiation in the XUV ( $10\text{-}300\text{ev}$ ) can be produced with laser intensities of  $10^{11}$  to  $10^{13}\text{Wcm}^{-2}$ . Although some experiments have been performed with  $10.6\mu$  radiation, most work to date has been done with  $1.064\mu$  and  $.694\mu$  sources. It is expected that excimer sources from  $200\text{nm}$  to  $350\text{nm}$  will also prove to be useful drivers. Typical driving laser energies range from  $10\text{J}$  in  $20\text{ns}$  for ruby and Nd:glass systems to  $1\text{mJ}$  in  $10\text{ps}$  for mode locked Nd:YAG lasers. With the use of Nd:YAG lasers the repetition rates are typically  $10\text{Hz}$  with pulse duration of  $10^{-11}$ - $10^{-10}$  sec for mode locked lasers and  $10^{-8}$  sec for Q switched lasers. The radiating source size varies from  $<50\mu$  for tightly focused, mode locked beams to  $\approx .2 - .5\text{mm}$  for longer duration pulses. The VUV output rises linearly with the incident laser energy at lower values and shows signs of saturation at higher energies. This feature means that the stability and reproducibility of the VUV output is at least as good as that of the driving laser.

If targets of low to moderate  $Z$  are used, then the emitted radiation consists of recombination and bremsstrahlung continua with intense line spectra superposed. In recent years it has been shown that if high  $Z$  targets are used then the complexity of states of the partially stripped ions produces such a multitude of lines that they merge into regions of continua which modulate the underlying recombination continua<sup>6</sup>. The result is not only an extremely clean spectra, essentially line free for as much as  $300\text{ev}$ , but a

concentration of intensity in limited regions of the XUV (see Figure 1).

The regions of intense emission can be varied by varying the target material.

The production of line free continua has been shown to be greatly enhanced by observing the source with focusing optics which select out the high density, high temperature core of the radiating plasma<sup>7</sup>. Calibration studies of laser plasma XUV sources are still underway but measurements of the absolute intensity of the sources indicate absolute conversion efficiencies from the driving radiation to blackbody radiation in excess of 5%<sup>5</sup>.

The use of high repetition rate lasers allows the construction of light sources which for many purposes are quasi-continuous. The irradiation of the target causes rapid erosion of the material as a crater is focused, the rate of erosion depending sensitively on the target material, but the area of damage is comparable to the laser spot size. Targets can be mounted on a rotating threaded shaft which presents fresh material to the laser after a fixed number of shots<sup>8</sup>. For systems which erode more slowly such as W or Cu, ten or more shots can be made at each position and it becomes feasible to construct a compact system which would run  $10^6$  shots before changing target material. An alternative approach has been demonstrated by Jopson et al.<sup>3</sup> where liquid Hg was used as the target material so that there was no cumulative target damage. A more serious problem for multiple exposures is the accumulation of spattered debris on optics and other surfaces. Incoming laser surfaces can be shielded by use of movable thin plastic films but this is obviously not feasible for regions exposed to XUV radiation. Kuhne et al.<sup>4</sup> and Carroll et al.<sup>6</sup> showed that laser plasmas can be operated with an ambient background gas which transmits the radiation of interest and Jopson et al.<sup>3</sup> used a He background pressure to protect their optical system from spattered Hg from their target.

## Sources of Radiation $\approx 300\text{ev}$

The use of moderate power lasers ( $\lesssim 10^9\text{W}$ ) is a convenient source of emitting plasmas but the electron temperatures are typically less than  $100\text{ev}$ <sup>(9,5)</sup>. The output for a  $100\text{ev}$  blackbody peaks near  $200\text{ev}$  and outputs fall rapidly at higher energies. For the production of x-ray photons it is necessary to go to larger power densities associated with very high energy, short pulse lasers which are usually associated with National laboratories, both here and abroad, and some large industrial efforts. The x-ray emission has been studied with sophisticated diagnostics and computer modeling capabilities so that it is better understood than the XUV radiation. The spectrum is predominantly free-free and free-bound radiation combined with a simple line spectrum. The heating mechanism for these high power lasers is inverse Bremsstrahlung which typically produces a hot, dense plasma with a density around  $10^{21}\text{ cm}^{-3}$  and an electron temperature of  $300\text{ev}$  to  $500\text{ev}$ . The plasma is characterized by transient stages of ionization before the ionization stages come to equilibrium. During subsequent times there is rapid ion movement due to expansion. The preponderance of electrons are Maxwellian and provide radiation of a few  $\text{kev}$ <sup>10</sup>. There is generally also a tail of hot electrons with energies up to several  $\text{kev}$  with radiation produced out to  $350\text{ kev}$ <sup>11</sup>. An experimental and theoretical study of laser plasmas with high time resolution has recently been reported by Nakano and Kuroda<sup>17</sup>. Their work not only covers the features mentioned above (except for the hot electrons) but also explains the strong dependence of electron temperature, and subsequent soft x-ray emission, on the  $Z$  of the target material.

Several studies have been made of the absolute conversion efficiency from laser input energy to x-ray photons. Matthews et al.<sup>10</sup> of Lawrence Livermore Laboratories have made such measurements with  $1.06\mu$ ,  $0.53\mu$ , and

0.35 $\mu$  radiation using intensities between  $10^{14}$  and  $10^{16}$  W cm $^{-2}$  with durations between  $10^{-10}$  and  $2 \times 10^{-9}$  sec. Targets of Al, Au, Ti, Ni and Zn were used, generating intense radiation between 2 and 10 keV with a strong, simple line spectrum on top of a continuum background (see Figure 2). The efficiency defined as the ratio of x-radiation to incident laser energy was independent of spot size (total energy) if pulse duration and intensity were constant. The efficiency decreased with increasing intensity and for Al and Ti targets was five times higher for .35 $\mu$  radiation than for 1.06 $\mu$  radiation. For intensities above  $3 \times 10^{15}$  W cm $^{-2}$  the efficiency was constant from  $10^{-10}$  sec to  $2 \times 10^{-9}$  sec. using 1.06 radiation. For the  $10^{-10}$  sec pulses the line output had a duration of 1.4 to 2.4 times the laser pulse duration, varying with the target, while the continuum output had approximately the duration of the laser. For  $6 \times 10^{-10}$  sec. pulses the line emission followed the laser.

Yaakobi et al.<sup>13</sup> at the Rochester Laboratory for Laser Energetics have made similar studies but find a significantly stronger increase in efficiency in going from 1.06 $\mu$  to 0.35 $\mu$  radiation. For a constant pulse duration they report that the x-ray output depends almost exclusively and linearly on the laser pulse energy. Defocusing to decrease the irradiance by more than a factor of 10 causes a decrease in efficiency of less than 1.5. The radiation temperature of the plasma was 0.8 keV for the continuum and 2 keV for the line emission. For a glass (Si) target with a  $5 \times 10^{14}$  W cm $^{-2}$ ,  $5 \times 10^{-10}$  sec driver laser the output was  $2 \times 10^{15}$  photons in the continuum and an approximately equal amount in the  $1s^2 - 1s2p$  resonance line. The efficiency into individual lines in the 1.8 to 7.8 keV region was between 0.1% and 1% into each line.

Nagel et al.<sup>14</sup> used lasers at 10.6 $\mu$ , 1.06 $\mu$  and 0.694 $\mu$  with 20 to 10 J in 20 ns to 40 ns pulses to study x-ray emission. The 1.06 $\mu$  laser was at

least 10 times more efficient than the  $10.6\mu$  laser. With a 40ns pulse the x-ray intensity scaled with energy as  $E^n$  with  $n \approx 2.5$  to 3. The maximum efficiency into the 1 to 3 keV region was 10%. Gilbert et al.<sup>15</sup> made similar studies on the effect of target material on x-ray generation. They studied 36 elements between Be and U using a  $1.06\mu$  laser generating 28J in 8ns focused to  $4 \times 10^{13} \text{ W cm}^{-2}$ . They observed an electron temperature of 365eV with an efficiency into 0.7 - 20keV photons which depended on Z but had a maximum value of 9.6%. The same efficiency was observed with a 1ns laser pulse. The use of a  $100\mu$  focal spot resulted in a  $120\mu$  emitting region. When U was used as a target no line emission was observed superposed on the continuum at energies above 800eV using a crystal spectrograph. Nakano and Kuroda<sup>12</sup> have studied x-ray emission using 2J of  $1.06\mu$  radiation and have also discussed the large variation of x-ray output with target Z. The atomic number for maximum output above >1keV was shown to be a function of the laser power density and the conversion efficiency into photons >1keV rose rapidly with the incident energy, reaching a maximum of  $2 \times 10^{-3}$  for 25J on target. The use of microballoon targets allows the achievement of higher electron densities ( $10^{23} \text{ cm}^{-3}$ ) and temperatures (1keV) than the use of flat targets<sup>13</sup>.

#### Absolute Intensities

Laser plasma outputs are most meaningfully compared with synchrotron radiation in the XUV where both sources provide a very clean continuum of radiation. Table 1 lists the results of measurements of absolute intensities from laser plasmas produced using conventional Nd and ruby laser of energy  $\leq 10\text{J}$ . The energy range of the measured photons varies from 10eV to 450eV and all measurements were made using grating spectrographs and monochromators. The measurements of Kuhue et al. (Ref 17) were in situ comparisons with a synchrotron radiation source, those of Mahajan et al. (Ref 7) were in situ

comparisons with a well characterized theta pinch and those of O'Sullivan et al. (Ref 18) were in situ comparisons with a calibrated standard arc lamp. The measurements of Nicolosi et al. (Ref 19) used a calibrated grazing incidence spectrometer and detector system while the oldest measurement, that of Breton and Papolar (Ref 20), used measured and estimated efficiencies for their spectrometer and photomultiplier. The measurements have all been put in the same units and the choices of parameterization are made to allow comparison of both the peak outputs and the average values (assuming 10 Hz operation) and of the intensity and the total flux output. The conditions of focus, temporal pulse behavior, incident angle on target, etc. are not standardized enough to make variations of factors of 2 meaningful. The values for synchrotron radiation sources are shown to give a sense of the comparability of the two sources.

The output of laser generated plasmas in the x-ray region involves strong line emission as shown in Fig. 2 from the work of Matthew et al. at the Livermore laser facility<sup>10</sup>. The dependence of the X-ray output as a function of incident power density is seen in Fig. 3 from Boobonneau et al.<sup>16</sup> using the third harmonic of a Nd:glass laser. One particularly interesting feature of this data is the crossing of the curves near 600eV so that in the XUV region an increase in laser power density decreases the radiant output in contrast to the behavior in the x-ray region. In addition to the thermal emission in the soft x-ray region, fast, suprathermal electrons in the laser driven plasma produce much harder x-rays. This is shown in Fig. 4 from Slivinsky<sup>11</sup>. Some of the many measurements of x-ray intensities are shown in Table 3 along with a comparison of the range of synchrotron radiation outputs.



comparisons with a well characterized theta pinch and those of O'Sullivan et al. (Ref 18) were in situ comparisons with a calibrated standard arc lamp. The measurements of Nicolosi et al. (Ref 19) used a calibrated grazing incidence spectrometer and detector system while the oldest measurement, that of Breton and Papolar (Ref 20), used measured and estimated efficiencies for their spectrometer and photomultiplier. The measurements have all been put in the same units and the choices of parameterization are made to allow comparison of both the peak outputs and the average values (assuming 10 Hz operation) and of the intensity and the total flux output. The conditions of focus, temporal pulse behavior, incident angle on target, etc. are not standardized enough to make variations of factors of 2 meaningful. The values for synchrotron radiation sources are shown to give a sense of the comparability of the two sources.

The output of laser generated plasmas in the x-ray region involves strong line emission as shown in Fig. 2 from the work of Matthew et al. at the Livermore laser facility<sup>10</sup>. The dependence of the X-ray output as a function of incident power density is seen in Fig. 3 from Boobonneau et al.<sup>16</sup> using the third harmonic of a Nd:glass laser. One particularly interesting feature of this data is the crossing of the curves near 600ev so that in the XUV region an increase in laser power density decreases the radiant output in contrast to the behavior in the x-ray region. In addition to the thermal emission in the soft x-ray region, fast, suprathermal electrons in the laser driven plasma produce much harder x-rays. This is shown in Fig. 4 from Slivinsky<sup>11</sup>. Some of the many measurements of x-ray intensities are shown in Table 3 along with a comparison of the range of synchrotron radiation outputs.

## Summary

Laser produced plasmas now exist as useable light sources in the XUV and soft x-ray region. The applications of the sources follow directly from the specific properties of the sources, namely that they are sources of radiation in the 10ev to 10 kev region with very high peak intensities and low duty cycles giving average output fluxes which can be comparable to synchrotron radiation source. The outputs are unpolarized, with a full illumination sphere, from a point source and they are highly reproducible, in contrast to pulsed electric arc or discharge sources. They can be run in the presence of significant pressures of background gas and impurities and, at least for XUV sources, are moderately priced, compact and easily portable.

In addition to being an intense source of XUV and soft x-ray radiation, laser produced plasmas have been shown to be as reproducible as the driving laser provided the target illumination and observation geometry are kept fixed. Thus they are very promising for the role of transfer standards, although it will probably be necessary to use single transverse mode, smooth pulse lasers as the driving source. Efforts are now going on to study the use of such plasmas as intensity standards in the XUV<sup>17</sup>. The compactness and modest cost of XUV systems make these a natural candidate for such applications. In contrast to synchrotron radiation sources, laser plasmas would provide intensity standards for high intensity, short pulse radiation and could be used to calibrate detectors for these conditions without the large extrapolations needed with calibration from low peak intensity sources. The suitability as standards is particularly apparent for sources below  $\approx 300\text{ev}$  where the laser plasma can produce a true continuum.

The continuum nature of the sources and their high reproducibility also make them excellent for spectroscopy while the high intensity between 200ev and

and 2 kev makes them well suited for materials application such as micro-lithography and the point source nature and toleration of ambient background gas make them well suited for x-ray microscopy. The high peak intensities are well suited for studying the interaction of intense burst of ionizing radiation with matter, including efforts to produce highly non-equilibrium conditions suitable for x-ray laser operation<sup>5</sup>. The high reproducibility under easily prescribed conditions make them excellent candidates for transfer standards in the XUV and soft x-ray regions.

Pulsed laser plasma light sources are still in need of extensive study to fully characterize their properties and optimize their outputs. However, sufficient work has been done since they were first observed twenty years ago to establish them as useful and sometimes essential sources for XUV and x-ray science.

This work was supported in part by the Air Force Office of Scientific Research under contract AFOSR 4900-83-C-0130.

## References

1. J. A. R. Samson, Techniques of Vacuum Ultraviolet Spectroscopy (Pied Publications, Lincoln, Neb.) 1967.
2. A. W. Ehler and G. L. Weissler, Appl. Phys. Lett. 8, 89 (1966).
3. R. M. Jopson, S. Darack, R. R. Freeman and J. Bokor, Opt. Letts. 8, 265 (1983).
4. M. Kuhne and J. -C. Petzold, Opt. Letts. 9, 16 (1984).
5. R. G. Caro, J. C. Wang, J. F. Young and S. E. Harris, Phys. Rev. A., 30, 1407 (1984).
6. P. K. Carroll, E. T. Kennedy and G. O'Sullivan, Appl. Opt. 19, 1454 (1980); G. O'Sullivan, J. Phys. B. 16, 3291 (1983).
7. C. G. Mahajan, E. A. M. Baker and D. D. Burgess, Opt. Letts. 4, 283 (1979).
8. G. O'Sullivan, P. K. Carroll, T. J. McIlrath and M. L. Ginter, Appl. Opt. 20, 3043 (1981); D. J. Nagel, C. M. Brown, M. C. Peckerar, M. L. Ginter, J. A. Robinson, T. J. McIlrath and P. K. Carroll, Appl. Opt. 23, 1428 (1984).
9. G. Tondello, E. Jannitti, P. Nicolosi and D. Santi, Opt. Comm. 32, 281 (1980).
10. D. L. Matthews, E. M. Campbell, N. M. Ceglie, G. Hermes, R. L. Kauffman, L. Koppel, K. Lee, K. Manes, V. Rupert, V. Slivinsky, R. Turner and F. Ze, J. Appl. Phys. 54, 4260 (1983).
11. V. W. Slivinsky in Low Energy X-ray Diagnostics, ed. D. T. Attwood and B. L. Henke (A.I.P., N.Y.) p. 6, 1981.
12. N. Nakano and H. Kuroda, Phys. Rev. A. 27, 2168 (1983).
13. B. Yaakobi, P. Bourke, Y. Couturie, J. Delettiez, J. M. Forsyth, R. D. Fankel, L. M. Goldman, R. L. McCrory, W. Seka, J. M. Soures, A. J. Burekand and R. E. Deslattes, Opt. Comm. 38, 196 (1981).
14. D. J. Nagel, R. R. Whitlock, J. R. Greig, R. E. Pechacek and M. C. Peckerar, SPIE Vol. 135, Developments in Semiconductor Microlithography III, p. 46 (1978).
15. K. M. Gilbert, J. P. Anthes, M. A. Gusinow, M. A. Palmer, R. R. Whitlock and D. J. Nagel, J. Appl. Phys. 51, 1449 (1980).
16. D. B. Babonneau, D. Billon, J. L. Bocher, G. Di Bona, X. Fortin and G. Thiell, presented at 6th Intl. Workshop on Laser Interactions and Related Phenomena, (Monterey, Calif., 25-29 Oct. 1982).

17. M. Kuhne and B. Wende in X-Ray Microscopy, ed. G. Schmahl and D. Rudolph (Springer-Verlag, Berlin) p. 30, 1984.
18. G. O'Sullivan, J. Roberts, W. Ott, J. Bridges, T. Pittman and M. L. Ginter, Opt. Letts. 7, 31 (1982).
19. P. Nicolosi, E. Jannitti and G. Tondello, Appl. Phys. B. 26, 117 (1981).
20. C. Breton and R. Papoular, J. Opt. Soc. Am. 63, 1225 (1973).

Ref	Laser Pulse Energy J	Measured Wavelength $\lambda$ (nm)	Peak Spectral Intensity Phot. sec <sup>-1</sup> MHz <sup>-1</sup> m <sup>-2</sup>	Average Spectral Intensity (10 Hz rep. rate)	Peak Spectral Flux Phot. sec <sup>-1</sup> MHz <sup>-1</sup>	Average Spectral Flux (10 Hz rep. rate)
20	10	121.6	$1.5 \times 10^9$	$1.5 \times 10^2$	$10^{16}$	$10^9$
7	2	121.6	$5 \times 10^6$	$5 \times 10^{-1}$	$3 \times 10^{13}$	$3 \times 10^6$
18	2.2	121.6	$10^7$	1.0	$6 \times 10^{13}$	$6 \times 10^6$
17	0.8	100	$3 \times 10^7$	3	$2 \times 10^{14}$	$2 \times 10^7$
17	0.8	15	$1.510^7$	1.5	$10^{14}$	$10^7$
17	0.8	6	$7 \times 10^5$	$7 \times 10^{-2}$	$4 \times 10^{12}$	$4 \times 10^5$
19	10	2.7	$6 \times 10^8$	$6 \times 10^1$	$4 \times 10^{15}$	$4 \times 10^8$
19	10	8	$6 \times 10^8$	$6 \times 10^1$	$4 \times 10^{15}$	$4 \times 10^8$
Characteristic Synchrotron Radiation Parameters						
Bending Magnets			$10^5 - 10^8$	$10^3 - 10^4$	$5 \times 10^6 - 5 \times 10^9$	$5 \times 10^4 - 5 \times 10^5$
Wigglers			$10^6 - 10^9$	$10^4 - 10^5$	$5 \times 10^7 - 5 \times 10^{10}$	$5 \times 10^5 - 5 \times 10^6$
Undulators			$10^7 - 10^{11}$	$10^5 - 10^8$	$5 \times 10^8 - 5 \times 10^{12}$	$5 \times 10^6 - 5 \times 10^9$

Table 1. XUV intensities and fluxes from laser produced plasmas. Synchrotron parameters are qualitative for comparison.

Ref	Laser Intensity $\text{W cm}^{-2}$	Laser Pulse Duration ns	Laser Pulse Energy kJ	Measured Output Photon Energy keV	Peak Spectral intensity Phot. $\text{sec}^{-1}$ $10\% \text{ BW } \text{mr}^{-2}$	Peak Spectral Flux Phot. $\text{sec}^{-1}$ $10\% \text{ BW}$
11	$3 \times 10^{14}$	2.2	4.1	40	$5 \times 10^{13}$	$3 \times 10^{20}$
11	$3 \times 10^{14}$	2.2	4.1	160	$5 \times 10^{12}$	$3 \times 10^{19}$
11	$3 \times 10^{14}$	2.2	4.1	350	$5 \times 10^{10}$	$3 \times 10^{17}$
10	$3 \times 10^{15}$	0.7	.6	1.8 - 3.6	$7 \times 10^{16}$	$4 \times 10^{23}$
13	$5 \times 10^{14}$	.5	.04 (.35 $\mu$ )	2.7	$2 \times 10^{17}$	$10^{24}$
15	$4 \times 10^{13}$	8	.028	1	$7 \times 10^{16}$	$4 \times 10^{23}$
<u>Synchrotron Radiation Sources</u>						
Bending Magnets						
				<100	$10^{14} - 10^{15}$	$5 \times 10^{15} - 5 \times 10^{16}$
Wigglers						
				<200	$10^{15} - 10^{16}$	$5 \times 10^{16} - 5 \times 10^{17}$
Undulators (projected)						
				<10	$10^{16} - 10^{19}$	$5 \times 10^{17} - 5 \times 10^{20}$

Table 2. X-Ray intensities and fluxes from laser produced plasmas.  
Synchrotron parameters are qualitative for comparison.

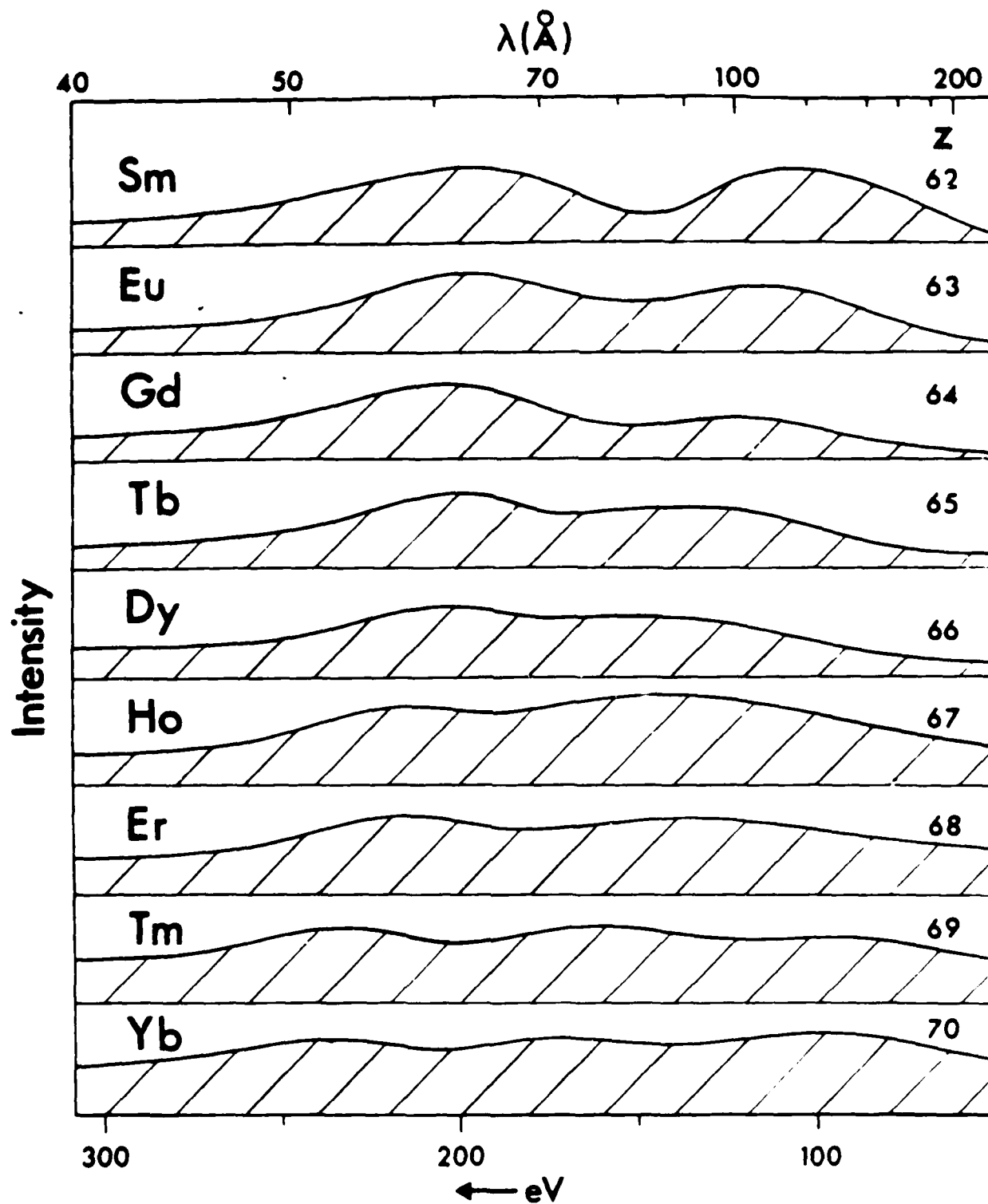


Fig. 1. Qualitative representation of continuum intensity distribution from laser produced plasmas using rare earth targets. From ref. 6.



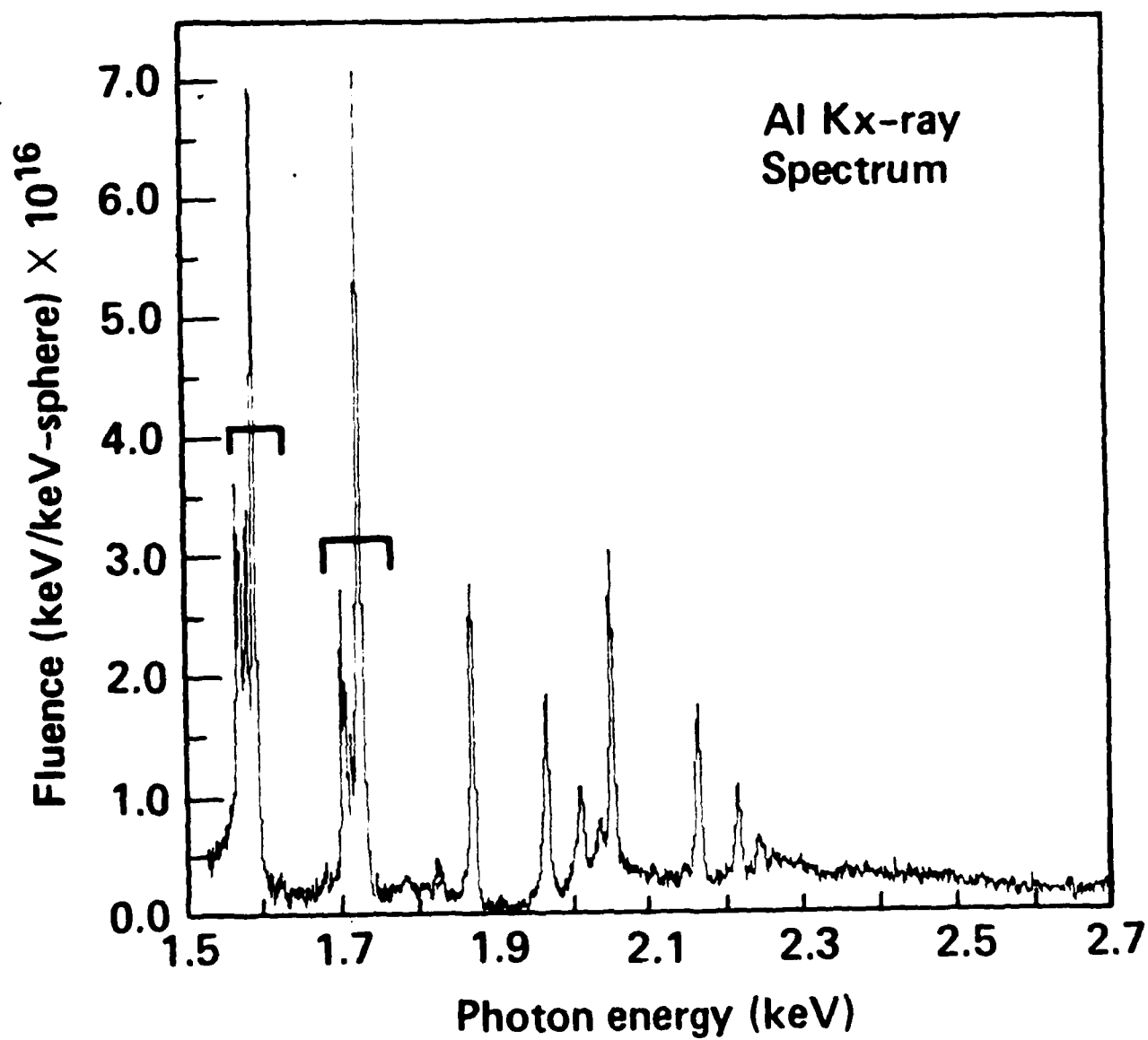


Fig. 2. X-ray intensity distribution from Al target.  
From ref. 10.

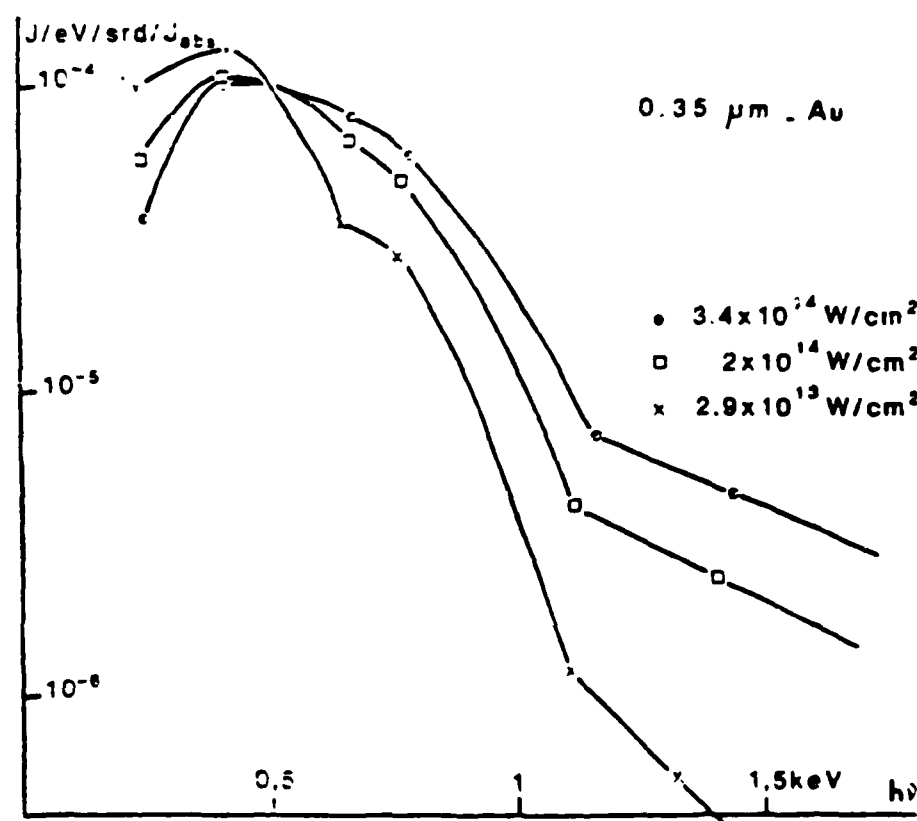


Fig. 3. Intensity distribution for different incident laser fluxes using Au target and .35 $\mu$  irradiation. From ref. 16.

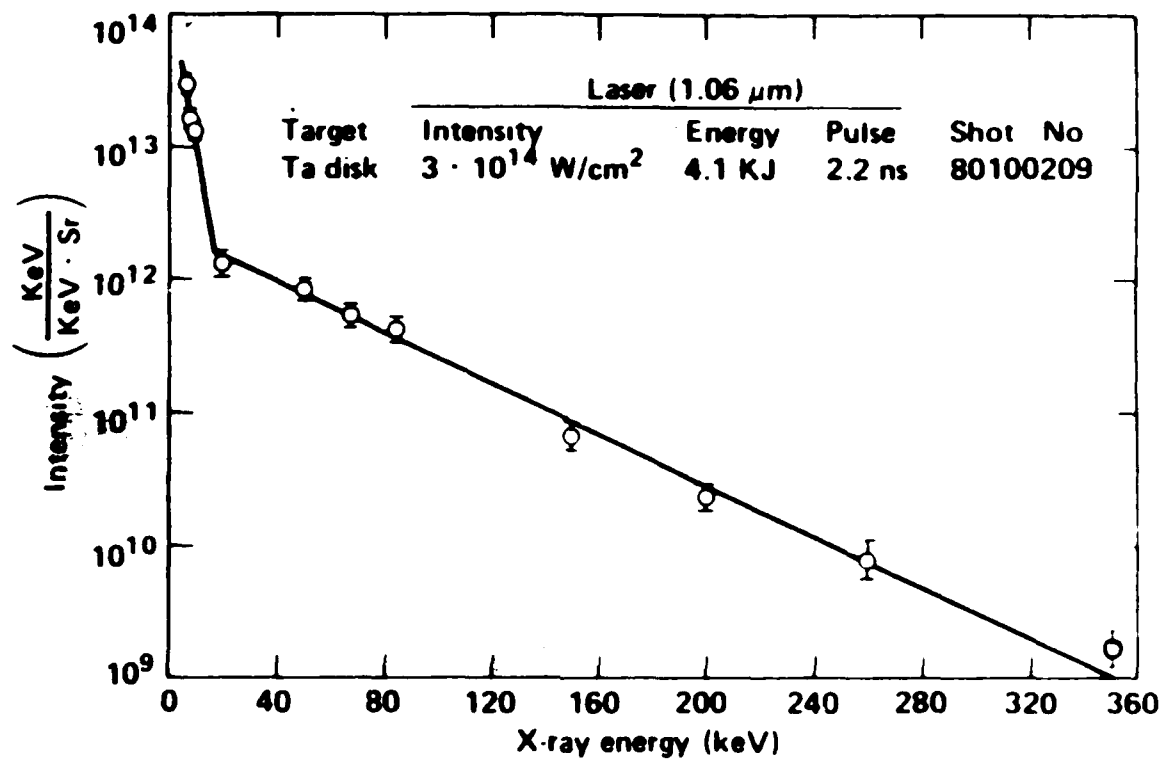


Fig. 4. Suprathreshold x-ray spectrum from a Ta target.  
From ref. 11.

## APPENDIX B

Abstract of a paper presented at the Eighth International Colloquium on  
Ultraviolet Spectroscopy of Astrophysical and Laboratory Plasmas

August 27-29, 1984

Washington, D.C.

XUV and soft X-ray radiation from laser produced plasmas as laboratory spectroscopic sources\*, P. Gohil, M.L. Ginter and T.J. McIlrath, Univ. of Maryland, IPST, College Park, MD 20742, H. Kapoor, D. Ma and C.M. Peckerar, U.S. Naval Research Laboratory, Washington, D.C. 20375. Laser produced plasmas have been shown to be excellent sources for applications in the XUV and soft X-ray spectral region.<sup>1</sup> We are using a 550 mj, 25 ns (FWHM) Nd:YAG laser operating at a repetition rate of 10 Hz to produce plasmas with rotatable solid targets.<sup>2</sup> The focal spot of the laser beam with a 31 cm lens was measured to be 170  $\mu\text{m}$  (approximately twice the diffraction limit), using a diode array having a 17  $\mu\text{m}$  resolution. Broadband output in the soft X-ray region was studied using a windowless PIN photodiode with an  $\text{Al}_2\text{O}_3$  surface covered with a polyethylene filter with transmission between 44  $\text{\AA}$  and 120  $\text{\AA}$ . Results are presented for the sources soft X-ray intensity for several elements as a function of laser energy, focus and driving wavelength as are preliminary results using the source for high resolution spectroscopy and for soft X-ray lithography.

\*Work supported by Air Force Grant AFOSR F49620-83-C-0130.

P. Gohil acknowledges support from SERC (UK).

1. Carroll, P.K., Kennedy, E.T. and O'Sullivan, G., 1980, App. Opt. 19, 1454.

2. Nagel, D.J., Brown, C.M., Peckerar, M.C., Ginter, M.L., Robinson, J., McIlrath, T.J., and Carroll, P.K., May 1984, App. Opt. 23.

Paper presented at SRI-85, Stanford, CA 9/21-1/2 (1985)

LASER PRODUCED PLASMA LIGHT SOURCES  
FOR HIGH RESOLUTION XUV AND VUV SPECTROSCOPY

M. L. Ginter and T. J. McIlrath  
Inst. for Phys. Sci. and Tech., Univ. of MD, College Park, MD 20742

Laser produced plasmas have been demonstrated to be convenient laboratory light sources for absorption spectroscopy below 500 Å.<sup>1</sup> It remained to be determined whether line structure would appear in apparent continua from these sources when observed at the highest possible spectral resolutions and whether such line structure would appear as the incident laser power is lowered. To answer these questions we have observed photographically the output from a laser plasma light source with W, Yb, or Cu targets (a) between 45 Å and 600 Å using the 10.6-m grazing incidence spectrograph at the National Bureau of Standards and (b) between 500-1100 Å using a 6.65-m normal incidence spectrograph at the University of Maryland.

The laser plasmas were produced at the 170 μm dia. focus of the output of a Nd:YAG laser (1.064 μ) using a 30 cm lens. For a typical laser pulse of 550 mJ in 25 ns, the maximum power density would be  $10^{11}$  W cm<sup>-2</sup> for the incident pulse. The cylindrical metal targets could be rotated to provide fresh material for every shot,<sup>2</sup> and the plasma was viewed at right angles to the incident laser beam with the normal to the surface at the focal spot being ~45° to both the laser beam and the viewing direction.

In the grazing incidence experiments, the target was 1-m from a focusing toroidal mirror which imaged the source onto the spectrograph entrance slit. The exposure times with Kodak 101-05 plates were typically 1-3 minutes (600-1800 shots) when the laser was operated at 10 Hz. Spectra using W and Yb targets appeared as extremely clean continua from 45 Å to 500 Å with no signs of line structure at the high resolution of our experiments. The continuum intensity dropped rapidly above ~500 Å and above ~550 Å the observed spectra were dominated by third order continuum emission, a feature used to record the absorption spectrum of the He  $1s^2 + 2snp$  autoionizing features at 190-207 Å in third order simultaneously with the principal series converging on the series limit at 504 Å (observed in first order). Even in the third order of the 10.6-m spectrograph no underlying structure was observed in these continua. In addition, the laser energy was dropped as low as ~100 mJ per pulse. Using the Yb target, 100 mJ pulses, and an increase in the exposure time by 5.5 gave photographic plate densities comparable to those obtained with 550 mJ pulses with no degradation in the uniformity of the continuum down to at least 80 Å. Examples of the photographically recorded high resolution grazing incidence spectra will be presented, as will similar results obtained with the 6.65-m instrument and additional applications of the light source.

The grazing incidence work was done with P. Gohil (Univ. of Md., College Park, MD) and V. Kaufman (National Bureau of Standards, Gaithersburg, MD). The normal incidence studies were done with F. Orth (Univ. of Md.). Work was supported by Air Force grant AFOSR F49620-83-C-0130.

1. Carroll, P. K., Kennedy, E. T., and O'Sullivan, G., Appl. Opt., 19, 1454 (1980).
2. O'Sullivan, G., Carroll, P. K., McIlrath, T. J., and Ginter, M. L., Appl. Opt. 20, 3043 (1981).

Reprinted from *Applied Optics*, Vol. 24, page 2024, July 1, 1985  
 Copyright © 1985 by the Optical Society of America and reprinted by permission of the copyright owner.

## Soft x-ray lithography using radiation from laser-produced plasmas

P. Gohil, H. Kapoor, D. Ma, M. C. Pekerar, T. J. McIlrath, and M. L. Ginter

Plasmas formed by focusing 0.6-J pulses from a 10-Hz Nd:YAG laser onto solid targets were used as soft x-ray sources for lithographic studies. Results of exposing masked photoresists to plasma radiation produced using steel, copper, and tungsten as targets are presented.

### I. Introduction

Laser-produced plasmas have proven to be excellent sources of short wavelength radiation with a wide variety of applications in the XUV and soft x-ray regions. In this work we report results which extend earlier<sup>1</sup> preliminary x-ray lithographic studies performed using a high-repetition-rate plasma light source.<sup>2</sup> The laser-driven light source and experimental chamber have been described in detail previously.<sup>1,2</sup> Briefly, the laser is an International Laser System (ILS) Nd:YAG laser ( $\lambda = 1.06 \mu\text{m}$ ), which consists of a Q-switched oscillator cavity and three amplifier sections operated at a repetition rate of 10 Hz. Laser pulses were 25-nsec FWHM with energies typically in the 630–670-mJ range for the majority of the experiments described below. The laser beam was steered to an evacuated source chamber by dielectrically coated mirrors and was focused on the surface of metal targets within an evacuated light source chamber by a convex glass lens with  $f = 310 \text{ mm}$  (see Fig. 1). Light emitted from the plasma produced by the focused laser pulse passes from the source chamber through an  $\sim 20\text{-mm}$  diam. aperture into an experimental chamber containing the object being irradiated, in the present case masked photoresist-coated substrates and/or x-ray photodiodes, with the

center line from the experimental chamber aperture to target being at nearly right angles to the laser beam (see Fig. 1).

### II. Experimental Conditions and Procedures

The irradiance of a driver pulse is determined from the laser parameters listed above and the focal spot size on the target surface. The focal spot size (focused beam waist) for the system in Fig. 1 was measured using a reticon diode array (resolution  $17 \mu\text{m}$ ) placed in the focal plane of the lens. To protect the reticon the incidence laser intensity was reduced  $\sim 10^{-7}$  by reflection of the beam off optical flats followed by passage through neutral density filters. The measured FWHM beam diameter was  $170 \mu\text{m}$ , as can be seen from the reproduction of a typical oscillograph of the reticon's output appearing in Fig. 2. Use of standard beam profile formulae for a  $\text{TEM}_{00}$  spatial mode<sup>3</sup> leads to a theoretical minimum spot size from our lens and laser of  $60 \mu\text{m}$  with a confocal beam parameter of  $14 \text{ mm}$ . Previous measurements<sup>1</sup> of target crater diameters for low-power pulses on refractory targets and on plastic tape provide an independent estimate of  $\sim 130 \mu\text{m}$  for the focal spot diameter. Since the  $\sim 170\text{-}\mu\text{m}$  images obtained on the reticon could be larger than the on-target images because of aberrations introduced by the intensity reduction optics (see above),  $170$  and  $60 \mu\text{m}$  seem reasonable upper and lower bounds, respectively. Thus, for 25 nsec, 0.65-J pulses with focal spot diameters of 60, 130, or  $170 \mu\text{m}$ , the averaged incidence irradiance on a target surface normal to the incident beam would be  $9.2 \times 10^{11}$ ,  $1.8 \times 10^{11}$ , or  $1.1 \times 10^{11} \text{ W/cm}^2/\text{pulse}$ .

The light source uses cylindrical metal targets ( $\sim 16\text{-mm}$  diameter) attached to a programmable stepping-motor-driven screw which can provide, among other options, a fresh area of target material for each laser pulse. The plasma-producing laser pulses usually are focused on the target surface somewhere in the octant between normal incidence ( $L$  in Fig. 3) and an in-

T. J. McIlrath and M. L. Ginter are with the University of Maryland, Institute for Physical Science & Technology, College Park, Maryland 20742 while M. C. Pekerar and D. Ma are with U.S. Naval Research Laboratory, Washington, D.C. 20375. P. Gohil is now with University of California, Lawrence Berkeley Laboratory, Berkeley, California 94720 and H. Kapoor is now with GTE Communication Systems, Reston, Virginia 22096.

Received 24 November 1984.

0003-6935/85/132024-00\$02.00/0

© 1985 Optical Society of America.

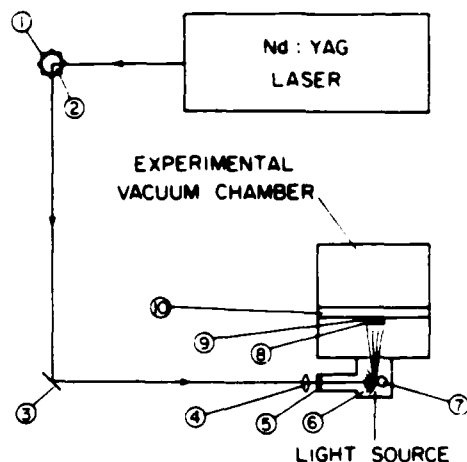


Fig. 1. Schematic diagram of experimental arrangements. Light from a laser is deflected and height adjusted with three mirrors (1,2,3) focused by a glass lens (4) through a Pyrex window (5) onto a cylindrical metal target (7) to produce a plasma plume (6). Radiation from the light source chamber passes into the experimental chamber through a mask (8) onto a photoresist-coated wafer (9) held in an alignment mount (10).

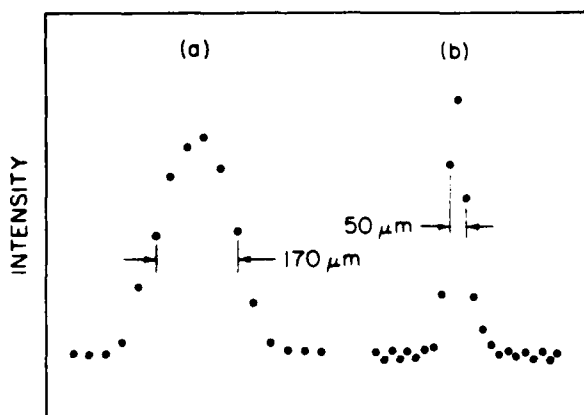


Fig. 2. Plots of the observed spatial distributions of the 1.064- $\mu\text{m}$  beam (a) and 0.6328- $\mu\text{m}$  reference beam (b) at the focus of an  $f = 310\text{-mm}$  lens. Data points are from 17- $\mu\text{m}$  wide detector elements on 17- $\mu\text{m}$  centers for 0.6328  $\mu\text{m}$  and from 17- $\mu\text{m}$  elements on 34- $\mu\text{m}$  centers for 1.064  $\mu\text{m}$ . Calculated values for  $2\omega_0$  ( $1/e^2$  full width) are 100  $\mu\text{m}$  (1.064) and 88  $\mu\text{m}$  (0.6328).

cidence angle of  $45^\circ$  to the target surface's normal ( $L''$  in Fig. 3). The choice of focal spot positioning on the target is determined by the experimental conditions desired, because both the intensity of the light and the quantity of ablation products from the target observed<sup>1,2,4</sup> in the direction of the experiment ( $E$  in Fig. 3) increase as the focused driver ray proceeds from  $L$  to  $L''$ . For the lithographic exposures described below, an angle of incidence of  $\sim 27^\circ$  ( $L'$  in Fig. 3) was chosen as a compromise between a reduced soft x-ray throughput to the wafer surface and an intolerable level of target debris in the experimental chamber containing the wafer. The elongation of the focal spot image in one direction produced by striking the target surface at  $27^\circ$  to the cylinder's normal leads to almost negligible de-

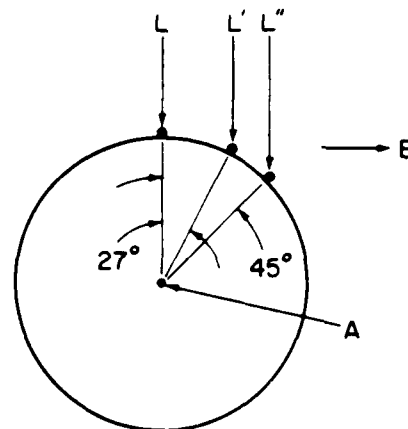


Fig. 3. Schematic diagram of laser focal spot positions on the target surface. The target cylinder rotates about axis  $A$ , which is perpendicular to incident laser rays ( $L, L', L''$ ) and to the plasma light exiting from the source to the experimental chamber in direction  $E$ .

creases in the averaged per pulse radiation discussed in the preceding paragraph (i.e., a drop from  $1.8 \times 10^{11}$  to  $1.6 \times 10^{11}$   $\text{W}/\text{cm}^2/\text{pulse}$  for the 130- $\mu\text{m}$  diameter normal incidence example, etc.).

Lithographic reproductions of circuit patterns were made by exposing masked photoresist-coated wafers placed  $\sim 15$  cm from the focal spot on the target to radiation from the plasma. The photoresist used was a copolymer of polyglycidyl methacrylate and ethyl acrylate (COP), which was spun to a thickness of 4700  $\text{\AA}$  on the surface of 76-mm diameter silicon wafers. COP is a negative photoresist with a sensitivity<sup>5</sup> of 15  $\text{mJ}/\text{cm}^2$  corresponding to the energy per unit area required to form bonds between molecules in the photoresist. Masks consisted of polyimide membranes overlaid with circuit patterns in gold.

The polyimide membrane used for mask construction was made by forming a thin layer of polyimide on a glass surface spinning at 4000–5000 rpm and by subsequent removal of the glass with hydrogen fluoride solutions. The transmission of the 1.5- $\mu\text{m}$  thick membrane was measured at the National Synchrotron Light Source (NSLS), Brookhaven National Laboratory, using the VUV storage ring. Using calibrated dosimeter film FWT 60-20,<sup>6</sup> the transmission, integrated over the  $\sim 44\text{--}100\text{-\AA}$  effective bandpass<sup>7</sup> of the membrane, was found to be 70%. To complete a mask, circuit patterns in a 0.5- $\mu\text{m}$  thick layer of gold were formed on the polyimide film.

In each experiment the photoresist-coated wafer was placed  $\sim 10$   $\mu\text{m}$  behind the mask in a kinematic mount designed to allow precise alignment of both mask and wafer. The mounted mask/wafer assembly then would be inserted in the experimental chamber and the light source and experimental chamber (see Fig. 1) evacuated to  $\sim 0.050$  Torr. Targets of copper, steel, or tungsten were used with the optical arrangements discussed above to expose the masked resists for times ranging from 15 to 60 minutes at pulse repetition rates of 10 Hz. After exposure, the mask and wafer were separated, the



Fig. 4. Photograph of a developed COP photoresist exposed through a mask for 1 h using a Cu target (see text). The smallest element is  $\sim 19 \mu\text{m}$  wide, while the small spots result from imperfections in the microscope optics and are not a product of the lithography.



Fig. 5. Photograph of a scanning electron micrograph of a developed COP photoresist exposed as in Fig. 4. The top figure is a  $\times 5$  enlargement of a portion of the lower panel, with the longer of the three white lines in the lower right-hand corner of the top figure being  $10 \mu\text{m}$  in the photograph. The small spots result from imperfections in the mask and not from the lithography.

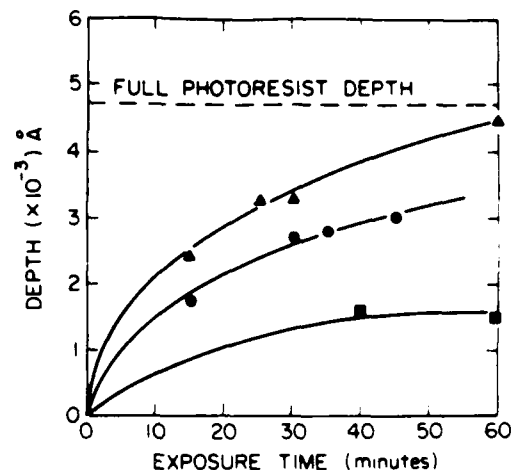


Fig. 6. Depth of photosensitized (etchable) resist as a function of exposure time to pulsed laser plasma radiation produced at a repetition rate of 10 Hz (see text). Triangles, circles, and squares represent data points for Fe (steel), Cu, and W targets, respectively.

exposed resist was removed from the wafer by developing, and the resulting lithographs were studied by detail.

### III. Results and Discussion

The developed photoresists were examined using both optical and electron microscopy. Figures 4 and 5 are reproductions of typical optical and electron microscope photographs, respectively, illustrating the clarity of sidewall profiles (average vertical wall uniformity better than  $0.3 \mu\text{m}$ ) obtained from lithographs in COP resists exposed using a copper target. The small spots in Fig. 4 result from dust particles in the microscope optics while the small indentations apparent in Fig. 5 result from pinholes in the mask. The depth of the resist removed on development corresponds to the depth photosensitized and, therefore, to the amount of radiation received by the resist which is effective in bond formation. The depths of development of photoresists exposed for different times using Cu, Fe (steel), or W targets were measured with an electron microscope, and the results are summarized in Fig. 6.

The radiations observed from the plasma source and targets employed in this work are most intense in the  $\sim 30$ – $500$ -Å region,<sup>1,8,9</sup> so that it seems likely that resist exposures resulted primarily from radiation transmitted in the short-wavelength ( $\sim 44$ – $100$ -Å) effective bandpass (see above) of the polyimide mask substrate. In these wavelength regions, the emissions from Cu and Fe (steel) targets are predominantly dense line spectra overlaying weaker continua (spectra of focused plasmas from Cu targets become predominantly continuous near  $50 \text{ Å}$ ) while the emissions from W targets are almost exclusively continuous with very few discrete spectral lines observable.<sup>1,8</sup> As can be seen from Fig. 6 it appears that radiation from Cu and Fe (steel) targets is at least twice as effective in exposing our masked COP lithographs as the continuous emission from W, with Fe being slightly superior to Cu. The relative ordering of



$\text{Fe} > \text{Cu} > \text{W}$  for exposure efficiency may have a slightly greater spread than implied by Fig. 6, since the quantities of ablation products produced by these targets fall in the order  $\text{W} > \text{Fe} > \text{Cu}$ . Thus, a system which reduces or stops the migration of ablation products from the targets into the experimental chamber might lead to greater differences between the efficiencies of Fe and Cu, etc. than those reported in Fig. 6.

The same masks and similar COP-coated silicon wafers were exposed<sup>7</sup> at NSLS and developed by the same procedures as the lithographs discussed above. The sole object of these experiments was the direct comparison of analogous lithographs prepared using different light sources. We find that (1) the lithographs exposed using the plasma light source were uniformly exposed over their entire area while the lithographs exposed using the electron storage ring light source (NSLS) were much less uniform, (2) to produce exposures comparable with those obtained in the most intense positions of the beam from NSLS requires  $\sim 10$  times more elapsed time using the laser plasma source, and (3) there were no obvious differences in the quality of the lithographs (wall and surface uniformity, etc.) made using either light source.

The total soft x-ray output of the laser plasma light source currently in use can be increased (1) by increasing the repetition rate of the laser, (2) by using focusing optics with soft x-ray reflective coatings, (3) by increasing the energy per pulse at the same repetition rate, and/or (4) by reducing the quantity of ablation products from the target which travel to the experiment. All four of these approaches will be incorporated in future efforts to produce a laboratory light source for soft x-ray lithography which is at least as intense and of significantly better intensity uniformity per steradian than

can be obtained from the current generation of synchrotron light sources.

This work was supported in part by the Air Force Office of Scientific Research under contract AFOSR 4900-83-C-0130. P. Gohil acknowledges support from the Science and Engineering Research Council (UK) in the form of a postdoctoral research fellowship.

## References

1. D. J. Nagel, C. M. Brown, M. C. Peckerar, M. L. Ginter, J. A. Robinson, T. J. McIlrath, and P. K. Carroll, "Repetitively Pulsed-Plasma Soft X-ray Source," *Appl. Opt.* **23**, 1428 (1984).
2. G. O'Sullivan, P. K. Carroll, T. J. McIlrath, and M. L. Ginter, "Rare-Earth Plasma Light Source for VUV," *Appl. Opt.* **20**, 3043 (1981).
3. M. Kogelnik and T. Li, *Proc. "Laser Beams and Resonators," IEEE* **54**, 1312 (1966).
4. G. O'Sullivan, J. Roberts, W. R. Ott, J. Bridges, T. L. Pittman, and M. L. Ginter, "Spectral-Irradiance Calibration of Continuum Emitted from Rare-Earth Plasmas," *Opt. Lett.* **7**, 31 (1982).
5. G. N. Taylor, "X-Ray Resist Materials," *Solid State Technol.* **73** (May 1980).
6. *Radi-Chromic Reader* (Far West Technology, Goleta, Calif. 93077).
7. H. Kapoor, M.S. Thesis (Electrical Engineering), U. Maryland, College Park, Md. (1984).
8. P. Gohil, V. Kaufman, T. McIlrath, and M. Ginter, "Very High Resolution Photographic Studies of Continua from Laser Produced Plasmas Between 50 and 550 Å," *Appl. Opt.* (to be submitted).
9. M. Kuhne and B. Wende, "Spectral Radiant Power Measurements of VUV and Soft X-Ray Sources," *X-Ray Microscopy*, G. Schmahl and D. Rudolph, Eds. (Springer, Berlin, 1984), p. 30.

APPENDIX E

In press in Nucl. Inst. and Method.

Laser Produced Plasma Light Sources  
for High Resolution XUV and VUV Spectroscopy

M. L. Ginter and T. J. McIlrath

Institute for Physical Science and Technology  
University of Maryland  
College Park, MD 20742

ABSTRACT

Light from a laser produced plasma light source has been observed with the highest possible spectral resolution currently available in the 4-120 nm region. Plasma radiations observed from W, Yb, and Hf targets were found to be continuous with very few line emissions. Examples of highly resolved absorption spectra of He I and Ar I obtained using the plasma light source are presented.

Laser produced plasmas have been demonstrated to be convenient laboratory light sources for absorption spectroscopy below 50 nm [1]. While plasma emissions produced using rare earth (or heavier) elemental targets appeared to be predominantly continuous [1,2] (if viewing was restricted to the high density, high temperature focus region), it remained to be determined whether lines or other substructures would appear if the continua were observed at the highest possible spectral resolutions. To answer these questions we have observed (photographic detection) the output from a laser plasma light source [3] with (a) the 10.6-m grazing incidence spectrograph at the National Bureau of Standards in the 4.5-60 nm region and (b) the 6.65-m normal incidence instrument at the University of Maryland in the 30-120 nm region.

The plasmas were produced by focusing the output from a Nd:YAG laser (1.064  $\mu\text{m}$  output) to a spot about 170  $\mu\text{m}$  in diameter on a metal target using an  $f=30$  cm lens (see refs. [2] and [3] for details). For a typical laser pulse of 550 mJ in 25 ns, this spot size implies a maximum power density of about  $10^{11} \text{ W cm}^{-2}$ . The cylindrical metal targets could be rotated to produce fresh target material for every pulse, but for long exposures the targets generally were run in such a manner that most target areas were used for several laser pulses. The plasmas were viewed at right angles to the incident laser beam with the normal to the target surface at the focal spot being approximately  $45^\circ$  to both the incident laser beam and the viewing direction. Line emission from surface impurities was minimized by cleaning the surface with low energy, super-radiant pulses before taking the spectra.

A 10.7-m grazing incidence instrument with a 1200 grooves/mm grating was used in conjunction with a toroidal focusing mirror to study the short wavelength emissions from the plasmas (see Fig. 1). Exposure times with a 50  $\mu\text{m}$

slit on Kodak SWR plates typically were in the 10-180 second range (100-1800 laser pulses) when the laser was operated at 10 Hz. For comparison, about half the number of shots were needed to obtain similar exposures with a BRV spark source but, at one pulse every 20 seconds, the time required for an exposure was almost a factor of 100 longer. Emissions observed using W or Yb targets proved to be completely continuous in the 4.5-60 nm range studied, with very few emission lines (typically one every 2-3 nm). As is well known [1] these continua are most intense in the 10-20 nm region, and good exposures were obtained in the 6-25 nm region with W targets in 12 seconds (at 10 Hz and 640 mJ per pulse) with the 4.5-6 nm region weak but still usable. Exposures with Yb targets were similar, although exposures with Yb may require up to 50% more time to be comparable to W at the shorter wavelengths. To confirm that the observations were not predominantly of scattered light, the He I absorption spectrum was photographed in the 19-20.6 nm and 51-58.4 nm regions. During these helium absorption experiments, it was discovered that the source's continuum falls sufficiently rapidly in intensity above 50 nm that one can observe both the 51-58 nm spectrum and the third order of the 19-21 nm spectrum (first order near 60 nm) on the same exposures without order separation. The resolution in these third order absorption spectra is better than 0.001 nm, and the purely continuous nature of the Yb and W emissions in the approximately 20 nm region is confirmed to that level of observation. The reader is referred to reference [4] for details and additional experimental results obtained with this system.

A 6.65-m normal incidence instrument with a 4800 grooves/mm grating (gold coated) blazed near 90 nm was used in conjunction with a spherical focusing mirror (osmium coated) to study the longer wavelength emissions from Yb, W, and Hf plasmas (see Fig. 2). First order exposures with a 50  $\mu$ m slit on Kodak

SWR plates ranged typically from 3 mins at 50 nm to 20 mins at 120 nm when the laser was operated at 10 Hz, with appropriate increases in exposure times when working with narrower slits or higher spectral orders. Emissions observed using W or Yb targets proved to be completely continuous in the approximately 30-120 nm region studied with very few line emissions - results entirely analogous to the shorter wavelength studies just discussed. The intensities of the ~~continua~~ decrease rapidly with increasing wavelength, so that we were able to observe the helium absorption transitions near 51 nm in both first and second orders (plate factors of 0.03 nm/mm and 0.015 nm/mm, respectively). Fig. 3 contains reproductions of typical first and second order absorption spectra of He I near the lowest ionization limit while Fig. 4 provides a comparison of the absorption spectrum of Ar I observed near its lowest ionization limits taken with the plasma light source and with a helium (J. van Hopfield) continuum light source. The resolution in the second order absorption spectra is better than 0.001 nm, so the purely continuous nature of the Yb, W, and Hf emissions in the approximately 50 nm region is confirmed to that level of observation. The reader is referred to reference [5] for details and additional experimental results obtained with this system.

The work done on the 10.7-m and 6.65-m spectrographs were done in cooperation with P. Gohil and V. Kaufman, and with F. Orth and K. Ueda, respectively. This work was supported by the Air Force Office of Scientific Research under contract 4900-83-C-0130.

Copy available to DTIC does not  
permit fully legible reproduction

## References

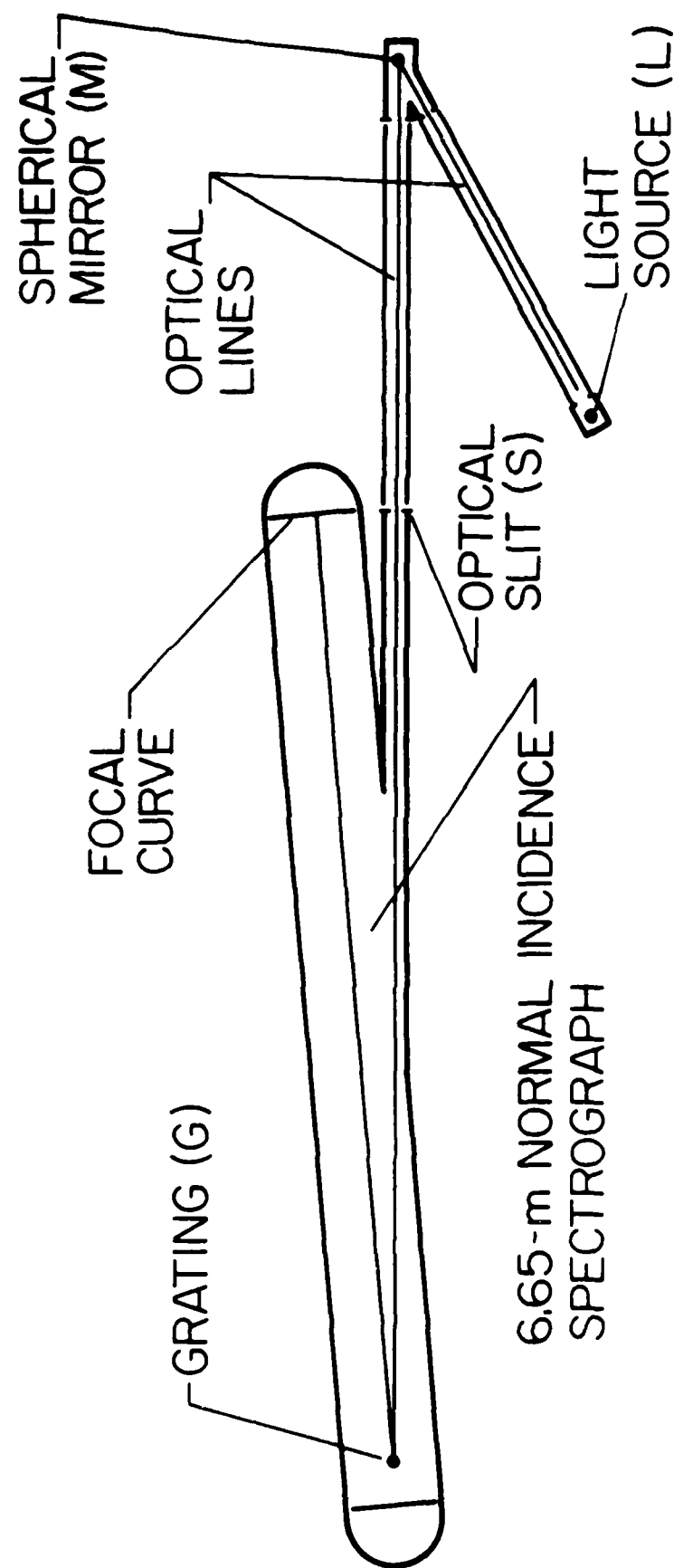
1. P. K. Carroll, E. T. Kennedy, and G. O'Sullivan, Appl. Opt. 19 (1980) 1454.
2. D. J. Nagel, C. M. Brown, M. C. Peckerar, M. L. Ginter, J. A. Robinson, T. J. McIlrath, and P. K. Carroll, Appl. Opt. 23 (1984) 1428.
3. G. O'Sullivan, P. K. Carroll, T. J. McIlrath, and M. L. Ginter, App. Opt. 20 (1981) 3043.
4. P. Gohil, V. Kaufman, and T. J. McIlrath, "High Resolution Spectra from a Laser Plasma Light Source in **the Grazing Incidence Region**", submitted to Appl. Optics.
5. F. B. Orth, K. Ueda, T. J. McIlrath, and M. L. Ginter, "High Resolution Spectra from a Laser Produced Plasma Light **Source** in the 30-120 nm Region", submitted to Appl. Optics.

### Captions to the Figures

- Fig. 1. Schematic diagram of the experimental arrangements used in the grazing incidence experiments. The distances between L and M and between M and S are 79 cm and 3 cm, respectively.
- Fig. 2. Schematic diagram of the experimental arrangements used in the normal incidence experiments. The distances between L and M and between M and S are 275 cm and 300 cm, respectively.
- Fig. 3. Absorption spectra of the He I near the 50.43 nm ionization limit in the first (a) and second (b,c) orders of a 6.65-m spectrograph using a 4800 grooves/mm grating and a laser driven plasma light source with a Yb target. Lines 1 and 2 are the  $1s^2\ ^1S-1s31p\ ^1P$  and,  $1s^2\ ^1S-1s14p\ ^1P$  transitions, respectively. Lines marked with an asterisk are impurities.
- Fig. 4. Absorption spectra of Ar I near 78 nm using a helium continuum (a) and a laser plasma with Yb target (b) as background light sources. The only difference is the impurity line indicated by an asterisk.





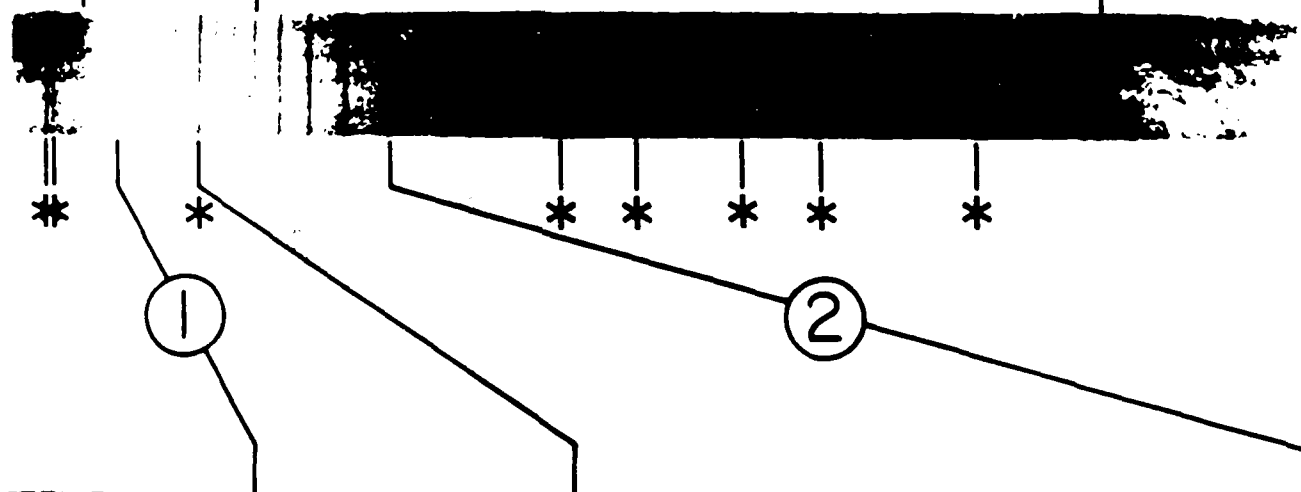


$1s^2 S$  LIMIT (50.43 nm)

(a)



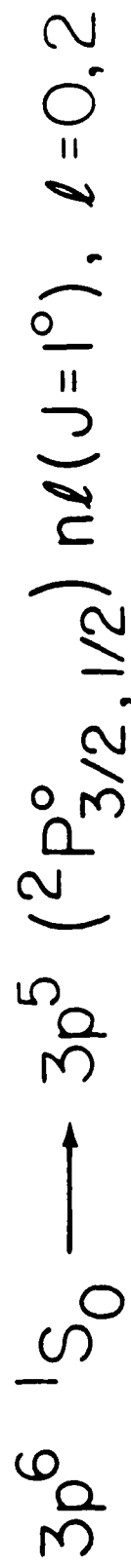
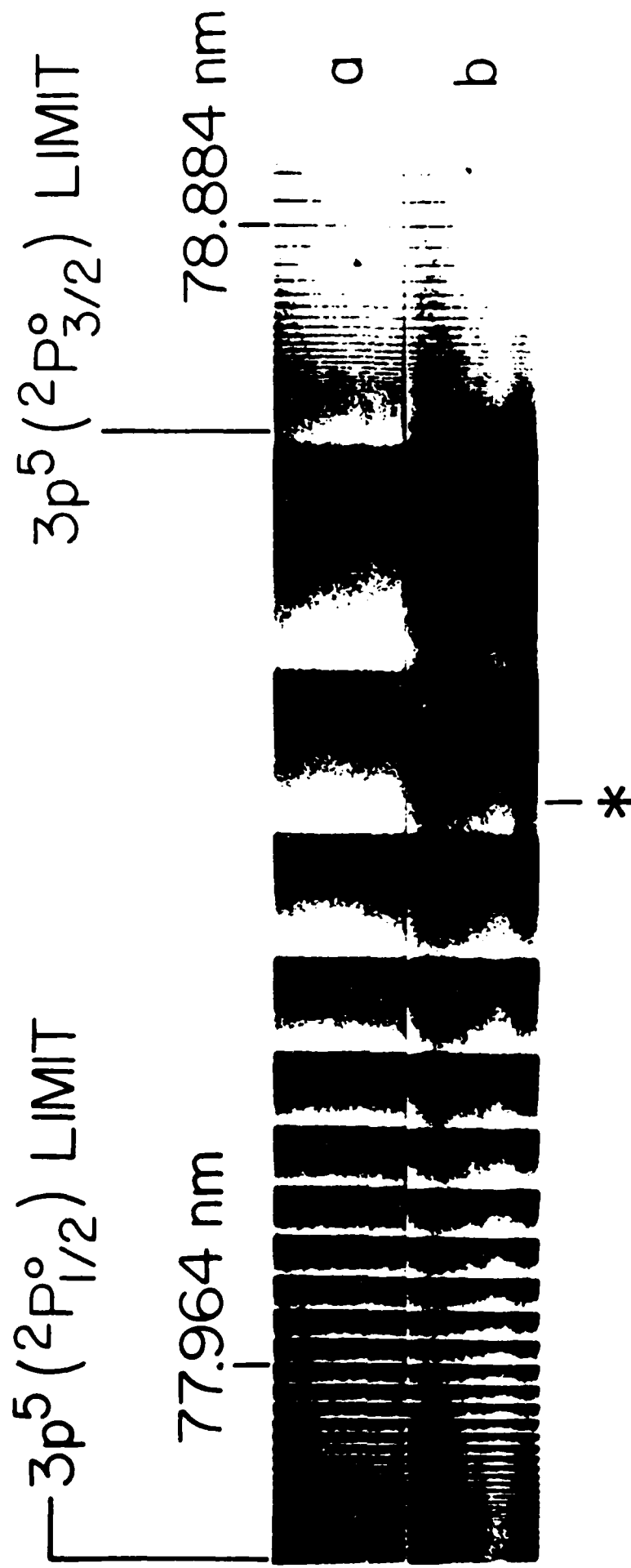
(b)



(c)



$1s^2 \ ^1S \rightarrow 1snp \ ^1P$  (He I)



## APPENDIX F

Submitted to Appl. Optics

### High Resolution Spectra of Laser Plasma Light Sources in the Grazing Incidence Region

P. Gohil, V. Kaufman, T.J. McIlrath

P. Gohil is currently at Lawrence Berkeley Laboratory, Berkeley, CA 94720  
V. Kaufman is at The National Bureau of Standards, Gaithersburg, MD 20899  
T.J. McIlrath is at The National Bureau of Standards and the University of  
Maryland, College Park, MD 20742

Recent studies of emission from laser produced plasmas have demonstrated their utility as sources of intense XUV and soft x-ray radiation.<sup>1</sup> In order to be useful as a laboratory spectroscopic light source, it is desirable that the source have high intensity, good reproducibility, and emit a clean continuum with a minimum of contaminating lines. Because the most promising targets are the high Z rare earth materials radiating from ionized systems with partially filled shells,<sup>2</sup> any line emission is likely to be extremely dense and easily confused, at low resolution, with continuum emission. In this paper we report on high resolution studies of emission from Cu, Yb, and W targets in the region from 45Å to 250Å. Even at the resolution of a 10.7 m grazing-incidence spectrograph ( $\Delta\lambda = .04$  Å) the Yb and W produce very intense and very clean continua in the 45Å to 250Å region. The Cu spectrum is heavily contaminated by emission lines at the longer wavelengths but produces a relatively clean continuum below 150Å.

The laser used in this experiment was a Nd:YAG producing a nearly diffraction limited beam at 1.064µm. The measured spot size using a single 300 mm focal length plano-convex lens was 170µm FWHM or approximately three times the diffraction limit. The laser pulse energy was ~630 mJ in 20 ns at a 10 Hz

repetition rate giving a power density on target of  $10^{11} - 10^{12} \text{ W cm}^{-2}$ , although one series of exposures was made with a single pulse energy of 100 mJ. The target was a cylindrical rod which was rotated between shots to provide a fresh surface on each shot. The incident laser beam and the viewing direction were orthogonal and the target normal was  $\approx 30^\circ$  from the viewing direction. Both the laser and the target chamber are described in more detail elsewhere.<sup>3</sup>

The target was placed 82 cm from the entrance slit to the spectrograph and focused onto the slit with an aluminized toroidal mirror placed  $\approx 3$  cm from the slit. The target surfaces were cleaned with a weak laser pulse before taking spectra in order to reduce emission from surface oxides. The target materials used were solid copper rod, sintered tungsten rod, and ytterbium sheet molded around a cylindrical center rod. The spectrograph was the National Bureau of Standards 10.7 m grazing-incidence photographic instrument with a 1200 g/mm grating and a 50  $\mu\text{m}$  entrance slit giving a resolution of  $\approx 0.04 \text{ \AA}$ . The spectra were recorded on 101-05 plates.

Sample spectra for copper, tungsten, and ytterbium targets are shown in Figure 1. The copper target gave an intense continuum, but it was heavily contaminated with emission lines above 150  $\text{\AA}$ . At shorter wavelengths, and especially below 100  $\text{\AA}$ , the emission is predominantly continuum. Because of their freedom from line emission most of our effort was spent on tungsten and ytterbium targets.

The W and Yb emissions were excellent sources of continua below 250  $\text{\AA}$ . The density of emission lines was typically one every 20  $\text{\AA}$  or 30  $\text{\AA}$  on the plate. In addition, the continuum was extremely intense. Good exposure were obtained in the 60  $\text{\AA}$  to 250  $\text{\AA}$  region with W targets in 12 seconds at 10 Hz and 640 mJ per

pulse delivering a total of 77 J to the target; exposures from 45 Å to 60 Å were weak but still useable at these energies. The continua from Yb targets were comparable in intensity, possibly requiring up to 50% more exposure time at short wavelengths. Both sources were comparable in the uniformity of the continuum.

One of the questions associated with the use of laser plasma light sources is how the character of the spectra changes with incident power density. In order to study this, we recorded Yb spectra with the laser intensity reduced by a factor of six to 100 mJ per pulse. Good exposures were obtained by increasing the exposure time by a factor of three. The spectrum was not visibly changed and there was no increase in line contamination. The one visible change was the apparent decrease in source size. This manifested itself most obviously in the 45-100 Å region where the spectrograph-toroidal mirror combination has a low astigmatism. This reduced source size probably accounted for the good exposures at half the delivered energy used at higher laser powers.

One feature of these sources is the localization of the output in broad spectral regions. In the case of Yb and W the outputs were especially weak above 500 Å. Part of this undoubtedly reflects the properties of the spectrograph. However absorption spectra of He were obtained and it was seen that most of the continuum observed in the region of 600 Å (first order) was in fact third order of the 200 Å emission. This is seen in Figure 2 where the 195 Å and the next four autoionizing resonances are observed in third order. The contrast across the line indicates the paucity of first order radiation. Second order radiation was presumably absorbed by the He continuum. The resolution in third order is  $\approx 0.1$  Å, and the purity of the continuum shown in this figure is typical of the Yb and W outputs. Figure 3 shows the absorption

spectrum of neutral He in the region above 500 Å.

To allow a comparison of intensities the same experimental set up was used with a BRV spark source to obtain exposures in the same spectral region. Exposures obtained with 150 shots, requiring 40 minutes, were significantly weaker than the laser plasma spectra and were not useable below  $\sim 1500$  Å. The BRV source also had considerable line emission overlying the continuum. The comparison is made more difficult by the wandering of the location of the BRV spark which spreads the short wavelength, stigmatic spectra over a considerably larger region of the plate than the laser source. Work with an imaging system on a normal incidence spectrograph (accompanying letter by Orth et al.) indicates that the ability to image a small, fixed region of the source onto the spectrograph entrance slit is an important factor in eliminating line emission.<sup>4</sup>

This work was partially supported by Air Force grant F49620-83-C-0130.

## References

1. See for example B.C. Fawcett, A.H. Gabriel, F.E. Irons, N.J. Peacock, and P.A.H. Saunders, "Extreme ultra-violet spectra from laser produced plasmas," *Proc. Phys. Soc. London* 88, 1051 (1966); A.W. Ehlers and G.L. Weissler, "Vacuum ultraviolet radiation from plasmas formed by a laser on metal surfaces," *App. Phys. Lett.* 8, 89 (1966); C. Breton and R. Papoular, "Vacuum-uv radiation of laser-produced plasmas," *J. Opt. Soc. Am.* 63, 1225 (1973); and P.K. Carroll and O'Sullivan, "Ground-state configurations of ionic species I through XVI for  $Z = 57-74$  and the interpretation of 4d-4f emission resonances in laser-produced plasmas," *Phys. Rev. A* 25, 275 (1982).
2. P.K. Carroll, E.T. Kennedy, and G. O'Sullivan, "Laser-produced continua for absorption spectroscopy in the VUV and XUV," *Appl. Opt.* 19, 1454 (1980).
3. G. O'Sullivan, P.K. Carroll, T.J. McIlrath, and M.L. Ginter, "Rare-earth plasma light source for VUV applications," *Appl. Opt.* 20, 3043 (1981).
4. F. Orth, K. Ueda, M.L. Ginter, and T.J. McIlrath, "High resolution spectra of laser-plasma light sources in the normal incidence XUV region," *Appl. Opt.* \_\_, \_\_ (19 \_\_).



## Figures

- Fig. 1 Spectra of (a) Copper 55 Å to 61 Å; (b) Tungsten 93 Å to 100 Å;  
(c) Copper 162 Å to 170 Å.
- Fig. 2 Absorption spectrum of He, 191 Å to 195 Å, taken in third order with a  
Ytterbium continuum and no order separator.
- Fig. 3 Absorption spectrum of He, 501 Å to 518 Å, taken in first order with a  
Ytterbium continuum.

(a)



55 Å   56 Å   57 Å   58 Å   59 Å   60 Å   61 Å

(b)



93 Å   94 Å   95 Å   96 Å   97 Å   98 Å   99 Å   100 Å

(c)



162 Å   163 Å   164 Å   165 Å   166 Å   167 Å   168 Å   169 Å   170 Å

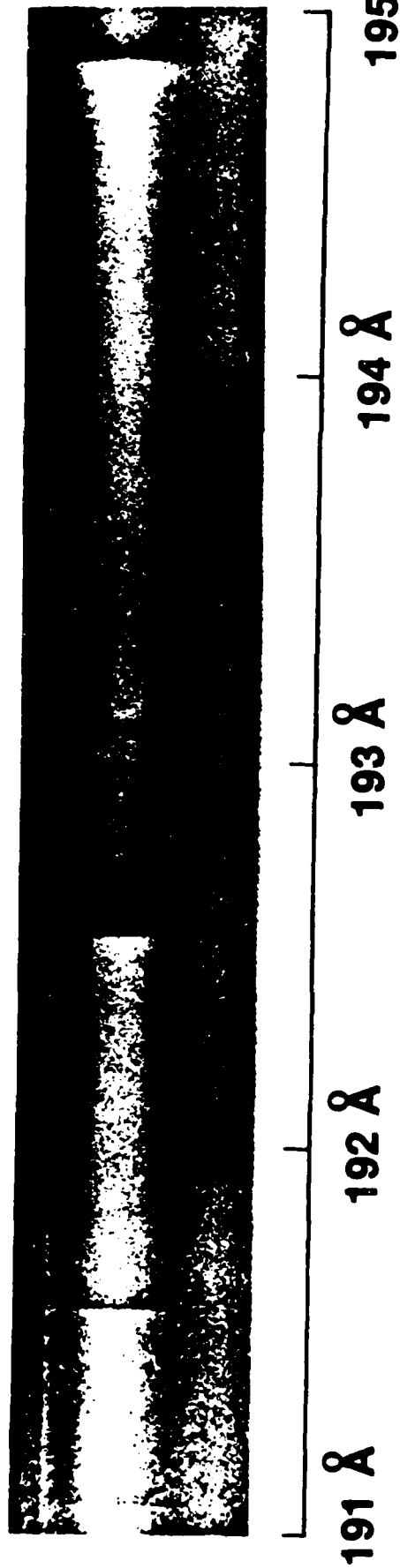


Figure 2

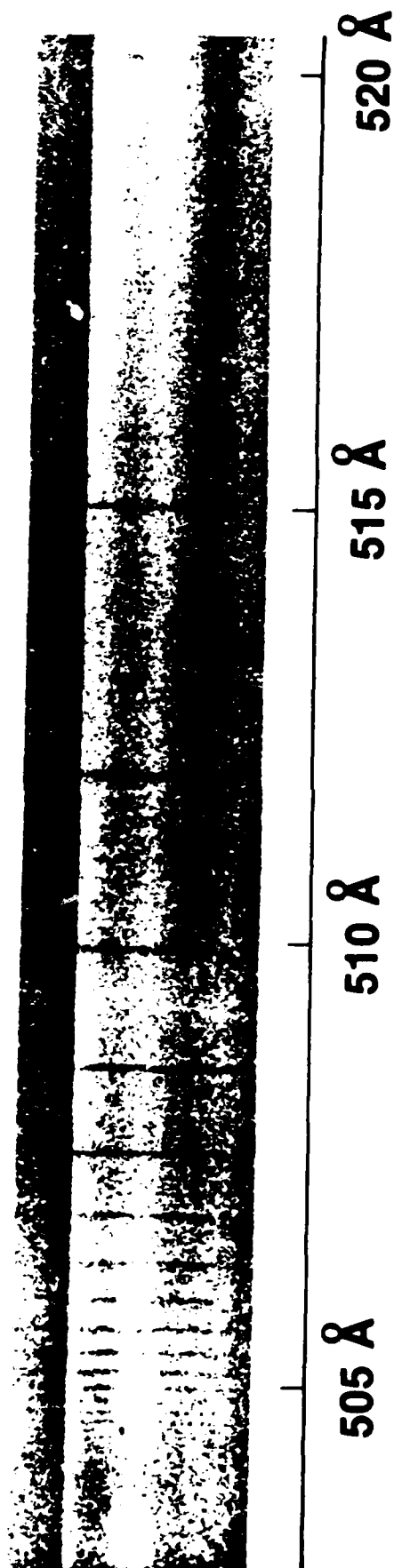


Figure 3

## APPENDIX G

### Preliminary draft of

#### Photoelectric Investigation of a Laser Produced Plasma VUV Light Source

J. M. Bridges, C. L. Cromer and Thomas J. McIlrath

#### Abstract

A photoelectric investigation was conducted on the XUV radiation from a laser-produced plasma. High-resolution, quantitative spectra from 7 to 40 nm were obtained from the plasma generated by a 0.5J Nd:YAG laser focussed on nine different target materials. The effects on the radiation of laser energy and quality of focus were measured. Some observations on target degradation and debris creation were also included, as well as some measurements using a 3J ruby laser.

## Introduction

When a pulsed laser is focused onto a solid target a dense, high temperature plasma is generated. Spectral line radiation as well as continuum radiation are generally emitted from such plasmas and their value as vacuum ultraviolet (VUV) and soft x-ray sources was recognized soon after the development of high power lasers. Early studies of laser produced plasma radiation concentrated on line emission originating from multiply ionized species. More recently, several studies have been directed towards the continuum radiation originating from inverse bremsstrahlung and recombination radiation and from a large number of blended spectral lines from targets having complex ionic configurations. Breton and Papolar<sup>1</sup> ~~et al~~ used both Nd:glass and ruby lasers with tantalum targets to produce intense radiation in the region of 121.5 nm including measurements of the absolute spectral intensity of the generated radiation, its angular distribution and its dependence on laser power. <sup>Bless and Nagel<sup>2</sup></sup> ~~Nagel et al~~ subsequently made extensive studies of the laser produced plasma radiation between 1.4 nm and 30 nm and the dependence of the radiation on the Z of the target. Several workers have extended the studies to the soft x-ray region and have used increasing powerful lasers to drive the plasmas.

Much of the work to date has been directed toward maximizing intensities over a broad spectral region and studies have been carried out with low spectral resolution, using target materials which yield a rich mixture of line and continuum radiation. Recent work by Carroll et al<sup>3</sup>, however, has included high resolution studies between 4 nm and 200 nm which have shown that with the proper choice of target material a virtually line free continuum can be produced over extended spectral regions.

The absolute spectral irradiances of laser produced plasma continua have been measured from 115-200 nm by O'Sullivan et al<sup>5</sup> and from 7-100 nm by Fischer et al<sup>6</sup>. These measurements also showed the irradiance to be quite reproducible, generally as good as or better than the driving laser. These factors have led to consideration of laser produced plasmas as background light sources for VUV spectroscopy and materials studies and as radiometric standards in the spectral region from 1 nm to 100 nm where no portable standards currently exist.

Further work is required however to establish the most effective sources for different spectral regions both in terms of spectral purity and maximum intensity, and to establish this type of source as an irradiance standard. In the present work, we report spectra between 7 nm and 40 nm obtained from nine target materials. In contrast to previous qualitative photographic observations or monochromator scans we have obtained photoelectric intensity measurements with high resolution. This was accomplished by the use of a recently constructed instrument using a photoelectric array detector. The measurements were made with a 0.5J, low divergence Nd:YAG laser and include investigations on the effect on the radiation of laser energy and quality of focus. In addition some measurements were made with a 3J ruby laser for comparison.

#### Experimental Arrangement

The details of most components of the apparatus have been described elsewhere<sup>6,7,8</sup> so that only a summary of the system is given here. The laser was a Q-switched Nd:YAG laser generating  $\approx 0.5J$  in  $\approx 25$  ns. The output was nearly a Gaussian in spatial extent with a focused spot size of approximately twice the diffraction limit in diameter. The radiation was focused onto the target with a 100 mm focal length plano-convex lens giving a measured focal spot diameter, full

width at half maximum, of 170 microns. Because of the possibility of aberrations introduced by the reflectors and the neutral density filters used in the measurement, this should be considered an upper limit with the diffraction diameter of 45 microns as a lower limit. Thus the peak power on target was  $10^{11} - 10^{12} \text{ Wcm}^{-2}$ .

The targets were cylindrical in shape, 15 mm dia X 6 mm long, mounted on a vertical threaded rod. After each laser pulse the target was moved to provide a clean surface for the following shot. In order to provide a comparison of the various target materials, several targets were mounted on the same shaft to allow the targets to be changed without breaking vacuum.

As shown in Figure 1, the incident laser beam was normal to the viewing axis with each axis being 45 degrees from the normal to the target material. The radiation from the target was viewed by the spectrometer<sup>19</sup> either directly through an entrance slit 50 cm from the target or by using a toroidal focusing mirror placed 10 cm from the spectrometer slit and used at 5 degrees incidence angle. The spectrometer was a 1.5 m grazing incidence instrument with a 1200 groove  $\text{mm}^{-1}$  grating. The detector assembly was mounted in<sup>2</sup>/<sub>chamber</sub> attached to the spectrometer scanning carriage in place of the normal exit slit and could be moved over the entire useable spectral region of the spectrograph without breaking vacuum. A zero-order trap and baffles were used to reduce zero-order and other scattered radiation.

The detector was a channel electron multiplier array (CEMA) which has been described in detail elsewhere.<sup>5</sup> The CEMA provides amplification into a phosphor which is connected to a self scanned diode array by a fiber optic bundle. The CEMA channels are separated by 15mm and the diode array elements are 25mm in width. Electron repulsion and imperfections in the fiber coupler limits the CEMA



spacial resolution to 1.2 pixels for a combined instrumental resolution of 0.01nm (or 3 pixels with 1200-line/mm grating and 10 $\mu$ m entrance slit). The output of the diode array was digitized and stored by a computer for processing. A spectrum was obtained with a single laser shot, but at least 20 shots were averaged to reduce the noise.

Structure in the output due to spacial gain variation across the CEMA was found to be  $\sim 20\%$  of full scale. It was determined that the gain profile was sensitive to the angle of incidence of the radiation, presumably because of changes in the penetration of the incident radiation into the micro channels. Thus it was impossible to measure the gain variation by uniformly illuminating the CEMA at normal incidence. The gain profile was determined by continuously scanning the CEMA carriage over a large spectral range while firing the laser and accumulating data. In this way each array element was exposed to approximately the same integrated spectral irradiance, at approximately the same angle of incidence. The accumulated gain profile was stored and used to divide into each measured segment of spectra, thereby eliminating apparent structure due to the gain profile itself.

To obtain the emission spectra for a given target material, the CEMA was successively placed in twelve overlapping positions to cover the entire 7nm  $\rightarrow$  40nm spectral range. For each position, the data from twenty laser shots were accumulated, detector background signal subtracted, and gain fluctuations divided out. The spectra for adjacent CEMA positions did not usually match perfectly in the overlapping regions because of laser power drifts and overall changes in CEMA efficiency with angle of incidence. Thus the relative normalization for each position was changed to match. This normalization process, combined with the spectral variation of the system efficiency precludes

drawing any conclusions concerning the relative intensities from any target material at different wavelengths, although relative intensities at a particular wavelength were obtained for all of the target materials and are accurate to better than 20%.

## Results

### a. Spectra

The spectra from the various targets are reproduced in Figure 2. The intensity scales at a given wavelength are the same for all materials. Significant differences between the various target materials are immediately apparent. Qualitatively they range from aluminum, which is predominantly <sup>2</sup>line spectra<sup>um</sup>, through samarium and ytterbium which are almost pure continua. Common lines in the samarium and ytterbium spectra at 225 Å and 170 Å are oxygen lines from surface oxide layers. In general the rare earths and tungsten give the cleanest continua in line with the reports of Carroll et al.<sup>3</sup> The rare earth continua show similar broad maxima with the peaks occurring at successively longer wavelengths with increasing Z as discussed by O'Sullivan.<sup>3</sup> The line spectra of aluminum and copper give good illustrations of the absence of second order spectra. The strong features at 160 Å in aluminum, for example are not seen at 320 Å.

### b. Intensities

The use of photoelectric detection with the CEMA, as opposed to photographic detection, provides accurate intensity information. Since our spectrometer system has not been calibrated, the data are valid only for relative intensities

and no absolute irradiance values can be given. Also, the variation with wavelength for each target reflects the wavelength response function of our system, but the sensitivity should vary slowly with wavelength so that local variations in intensity are accurately portrayed. Moreover, Fischer et al<sup>5</sup> have calibrated the spectrum from a tungsten target irradiated by a Nd:YAG-glass laser. Comparing our spectrum from a tungsten target with their calibrated spectrum should give a good estimate for the response of our system as a function of wavelength. Such a comparison indicates that our system has its peak efficiency at 19.0 nm, and drops off smoothly to a value of 0.2 times the peak efficiency at 11 nm on one side and at 40 nm on the opposite side. As mentioned previously, a toroidal mirror focused the radiation from the target onto the spectrometer slit. The mirror was used to increase the intensity at the slit to allow a smaller slit width and higher spectral resolution. For the tungsten target, a scan was also made with the mirror removed and direct irradiation from the target to the slit was used. For this condition the observed spectral distribution of the radiation was unchanged from the distribution observed using the mirror, showing that with tungsten targets the spectrum is not critically dependent on the observed area of the source. In fact, the difference in the observed areas of the source with or without the mirror is limited by the large astigmatism and aberrations of the toroidal mirror.

The data in Figure 2 shows the large enhancement in continuum intensity as the target moves to heavier Z. The most intense output was obtained using Hf, with Yb providing an excellent choice for high intensity and clean continuum. Samarium also produced good intensities above 250 Å with a greatly reduced output near 150 Å - 175 Å compared with Hf or Yb. The primary value of Al is seen to be

as a line source. Copper is strongly contaminated with lines but has a substantial underlying continuum, especially at short wavelengths. These results are consistent with the reports on photographic spectra by Carroll et al.<sup>4</sup> but give a quantitative measure of the relative intensities of different source materials.

### C. Dependence on focus and Laser energy

By moving the laser focusing lens along the optical path, the dependence of the signal on focus quality was measured. The result is shown in Figure 3 for a Ytterbium target with a wavelength bandpass of 3 nm center at 20 nm. In order to avoid the effects of small displacements of the imaged source relative to the spectrograph slit, the intensities for varying focus conditions were measured without the toroidal mirror. Similar results were obtained with the mirror in place, however.

The lens was a simple plano-convex, 100 mm focal length glass singlet and the measured focal spot diameter, full width at half maximum intensity, was 180 microns. The theoretical spot diameter for a diffraction limited beam is 45 microns and the confocal beam parameter is 12 mm. The data in Figure 3 was taken with a Yb target and the Nd:YAG laser at two different target positions along the laser axis. Both scans show a broad peak with a relatively narrow dip near its center. Figure 4 shows a similar scan using the ruby laser and a tungsten target. The results are qualitatively the same although the beam quality of the ruby laser beam is markedly inferior to that of the Nd:YAG laser. It is not clear what is the cause of the narrow intensity dip. At the best focus the power density on target is a maximum but the irradiated area is a minimum. It would appear that the maximum XUV intensity occurs with a larger than minimum emitting area and a reduced incident power density.

*Lower numbers on the lens position corresponds to focusing on target*

The dependence of the XUV output and spectra on Laser energy were investigated by varying the incident laser energy for fixed focus conditions. Figure 5

shows a plot of the integrated signal between  $18.5\text{ nm}$  and  $21.5\text{ nm}$  using a Yb target and Nd:YAG laser energies from 160 to 540 mJ. Two curves are shown, one for which the lens was positioned for maximum signal at 500 mJ incident energy and one with the lens positioned at the intensity dip shown in Figure 5. Both curves show a general linear dependence with an energy threshold but the two curves have different slopes. They cross at about 230 mJ so that the lens position giving a reduced output at higher energies gives a greater output at lower energies. This is consistent with the dip occurring at the position of best focus. The laser energy was varied in these experiments by varying the amplifier voltage while keeping the oscillator conditions fixed in order to minimize variations in beam character. Fig. 6 gives the results of some measurements of signal dependence on laser energy for the ruby as well as the Nd:YAG laser. These data are for XUV output near 18 nm from a tungsten target. The focus was adjusted for maximum signal for each laser. These data show the threshold VUV output using the ruby laser to be considerably higher than that using the Nd:YAG laser, and also show evidence of saturation at higher incident powers using the ruby laser. This again is in keeping with the interpretation of the focus behavior if the hottest part of the focused beam is above the point where the dependence on incident power becomes sublinear.

In order to study the effect of incident power on the spectral distribution of the output, Hf was irradiated at both 500 mJ and 200 mJ pulse energy. Figure 7 shows the ratio of the resulting spectra. (The spectra at 500 mJ is shown in Figure 2). It is clear that above 200 Å the spectra are essentially identical with an output proportional to the input energy. Below this wavelength there is a decrease in the relative intensity of the output in the 200 mJ incident spectrum indicating a faster than linear drop in output at short wavelengths.

There is no obvious increase in the line content of the spectrum at lower incident laser powers.

#### Target Debris

One of the major disadvantages of laser plasma sources is the production of large amounts of splattered material from the target. The Nd:YAG laser was operated at a 1 Hz repetition rate for the Q-switched pulse in order not to overload the data handling capabilities of the system, but with a 10 Hz repetition rate of the flash lamps in order to maintain a constant heat load on the laser system which was aligned at 10 Hz. On each of the 9 pulses which were not Q-switched a superradiant pulse of  $\approx 25$  microjoules and long duration was observed. Although the energy of the superradiant pulse was orders of magnitude less than the 500 mJ Q-switched pulse, it was found to produce comparable cratering on the target and to contribute comparable amounts of debris as the Q-switched pulse. Figure 8 shows target cratering for both the superradiant pulses and the Q-switched pulse. It was found that the use of a mechanical shutter to block the superradiant pulses significantly reduced the debris problem in the system. In <sup>addition</sup> ~~particular~~, it was found that if only the Q-switched pulses are allowed into the system, the incident laser pulse kept the central portion of the input window clean by burning off any accumulated debris with each shot.

Both the degree and character of cratering in the targets varied significantly between targets. The tungsten targets showed little damage but the debris had the character of the large particles. Copper targets also showed little observable target damage. The rare-earth targets showed deep cratering indicating significant melting of the material and the debris had the character of an evaporation source.

### Summary

We have made photoelectric studies of the XUV output of laser produced plasma light sources with high resolution in the spectral region 100 Å to 400 Å. Spectra have been obtained for Al, Cu, Fe, Sn, Sm, Hf, Yb, W, and Pb which can be directly compared for relative intensity at each wavelength. Several of the rare earths and Tungsten show very clean continuum outputs with little line contamination. The outputs were linear with incident laser energies up to greater than 1 J per pulse and the dependence of the output on focus conditions was shown to produce maxima away from the apparent point of minimum spot size. There was no significant degradation of the continuum nature of the spectra with decreasing laser energies down to 200 mJ per pulse. The target debris problem was seen to be manageable but the debris produced by low energy superradiant pulses was surprisingly high. In general, these sources seem to be fulfilling their promise as XUV laboratory light sources and seem to have all the required properties for secondary intensity transfer sources in the difficult XUV spectral region.

We gratefully acknowledge the assistance of D. Margon. The assistance of P. Gohil and the guidance and assistance of T.B. Lucatorto were essential in carrying out this work. This experiment was partially supported by Air Force Office of Scientific Research (AFOSR) contracts F49620-83-C-0130 and ISSA 85-0033.

## REFERENCES

1. C. Breton and R. Papoular, "Vacuum-uv radiation of laser-produced plasmas", J. Opt. Soc. Am. 63, 1225 (1973).
2. R. D. Bleach and D. J. Nagel, "Plasma X-Ray emission produced by ruby laser at  $10^{12}$  w/cm<sup>2</sup>", J. Appl. Phys. 47, 3832 (1970). See also K.M. Gilbert, J. P. Anthes, M. A. Gusinow, M. A. Palmer, R.R. Whillock and D.J. Nagel, J. Appl. Phys. 51, 1449 (19 ).
3. P. K. Carroll, E. T. Kennecey and G. O'Sullivan, "Laser-produced continua for absorption spectroscopy in the VUV and XUV", Appl. Opt. 19, 1454 (1980).
4. G. O'Sullivan, J. Roberts, W. R. Ott, J. Bridges, T. L. Pittman and M. L. Ginter, "Spectral-irradiance calibration of continuum emitted from rare-earth plasmas", Opt. Lett. 7, 31 (1982).
5. J. Fischer, M. Kuhne and B. Wende, "Spectral radiant power measurements of VUV and Soft x-ray sources using the electron storage ring BESSY as a radiometric standard source", Appl. Opt. 23, 4252 (1984).
6. D. J. Nagel, C. M. Brown, M. C. Peckerar, M. L. Ginter, J. A. Robinson, T. J. McIlrath and P. K. Carroll, "Repetitively Pulsed-Plasma Soft X-ray Source", Appl. Opt. 23, 1428 (1984).
7. G. O'Sullivan, P. K. Carroll, T. J. McIlrath and M. L. Ginter, "Rare-Earth Plasma light source for VUV", Appl. Opt. 20, 3043 (1981).
8. C. L. Cromer, J. M. Bridges, J. R. Roberts and T. B. Lucatorto, "A High-resolution VUV Spectrometer with Multichannel Detector for Absorption Studies of Transient Species",
9. Gerard O'Sullivan, "The Origin of Line-free XUV Continuum emission from laser-reproduced plasmas of the elements  $62 \leq Z \leq 74$ ", J. Phys. B 16, (1983).



Resolution = 0.1 eV

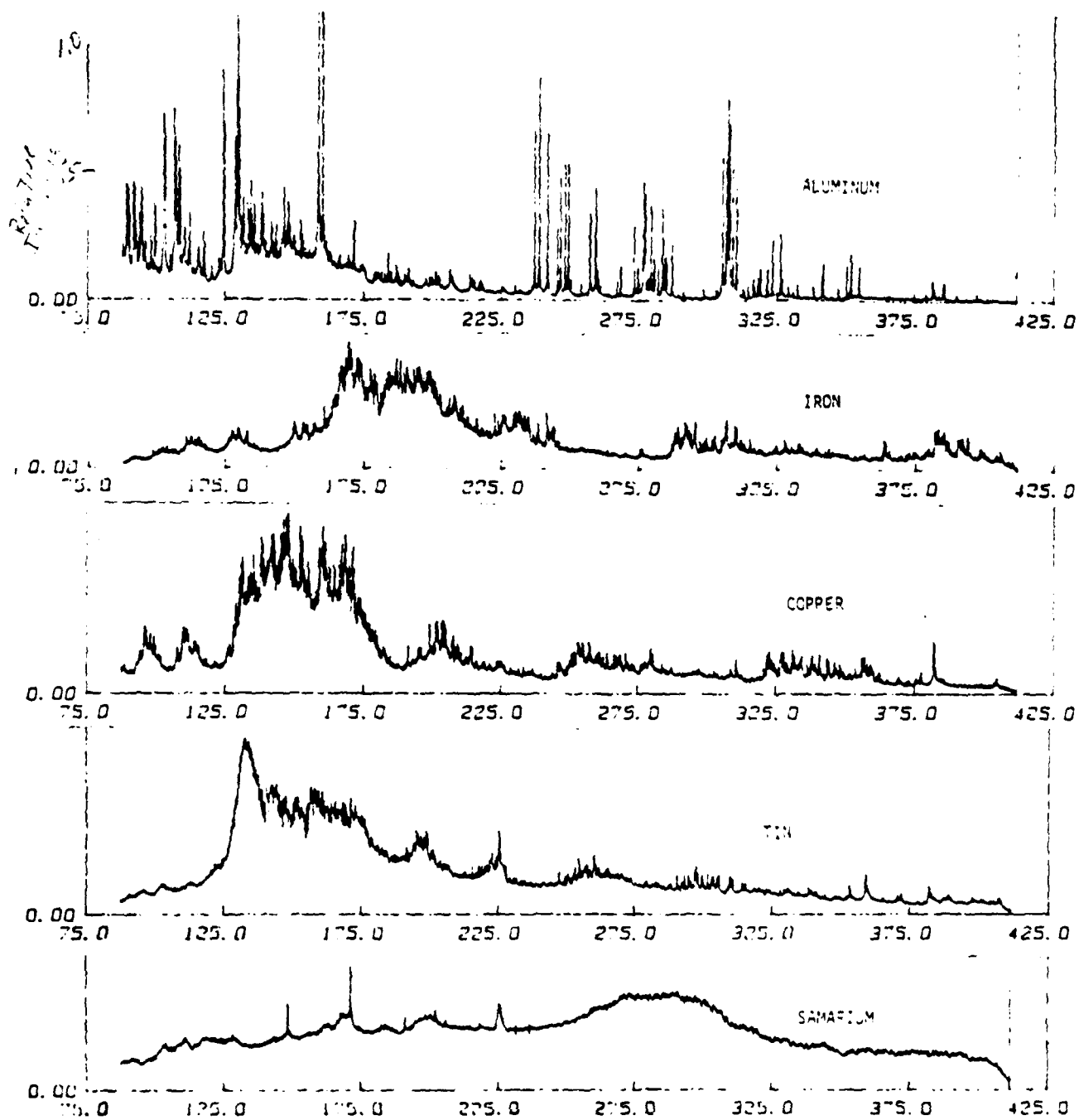


Fig 2

Spectra of the sample

### Figure Captions

Fig. 1. Diagram of target alignment.

Fig. 2. Spectra from various target materials.

Fig. 3. Dependence of signal on focus quality (Nd:YAG laser).

Fig. 4. Dependence of signal on focus quality (Ruby laser).

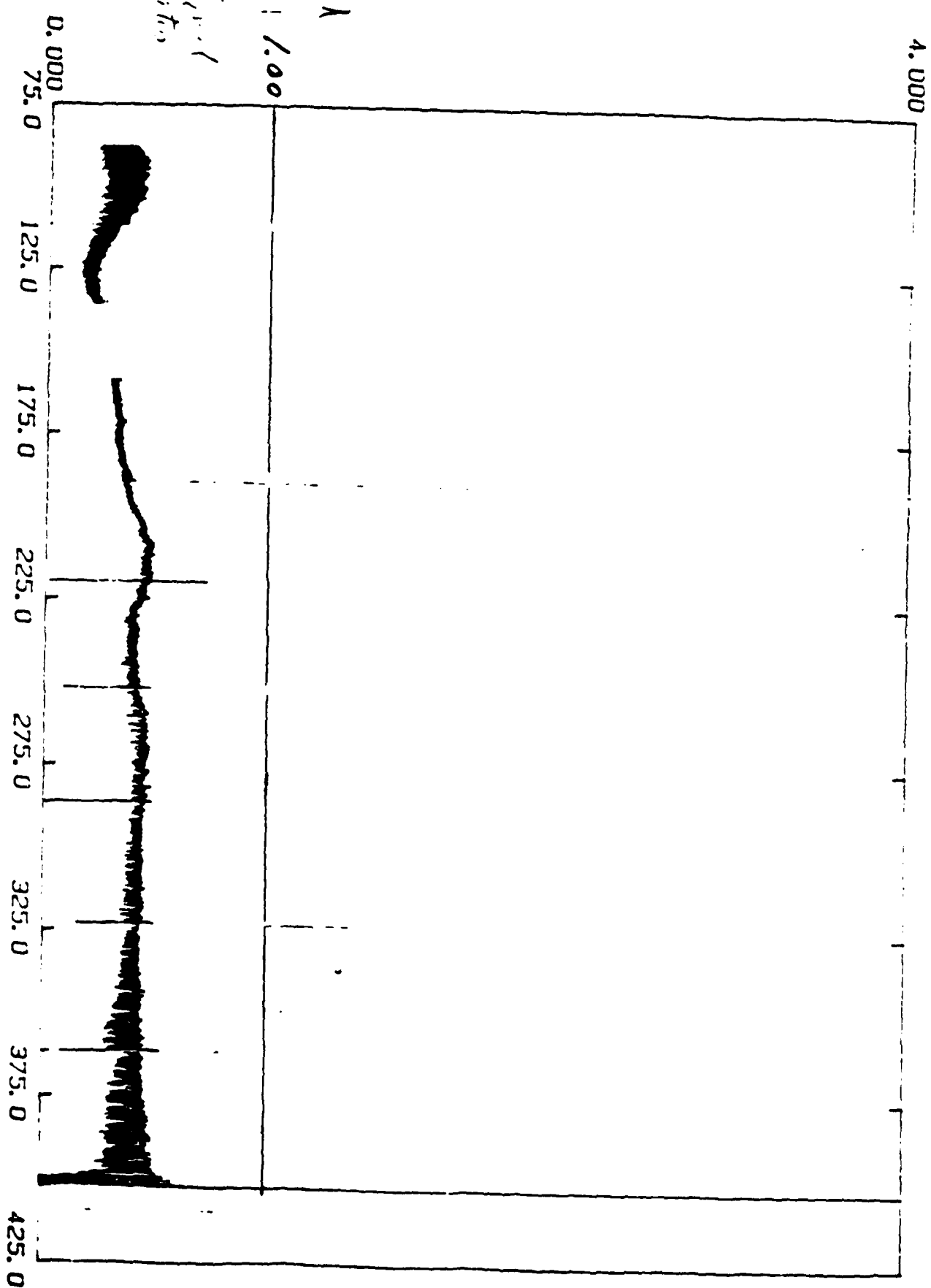
Fig. 5. Signal vs Laser Energy. Nd:YAG laser on Ytterbium target;  $\lambda = 20$  nm.

Fig. 6. Signal vs Laser Energy. Nd:YAG and Ruby Lasers; tungsten target,  $\lambda =$ .

Fig. 7. Ratio of signals from Hf target, for laser energies of 200 mJ and 500 mJ respectively.

Fig. 8. Target damage for four target materials.

Copy available to DTIC does not  
permit fully legible reproduction



1891

Y

1.00

0.000

75.0

125.0

175.0

225.0

275.0

325. U

**375.0**

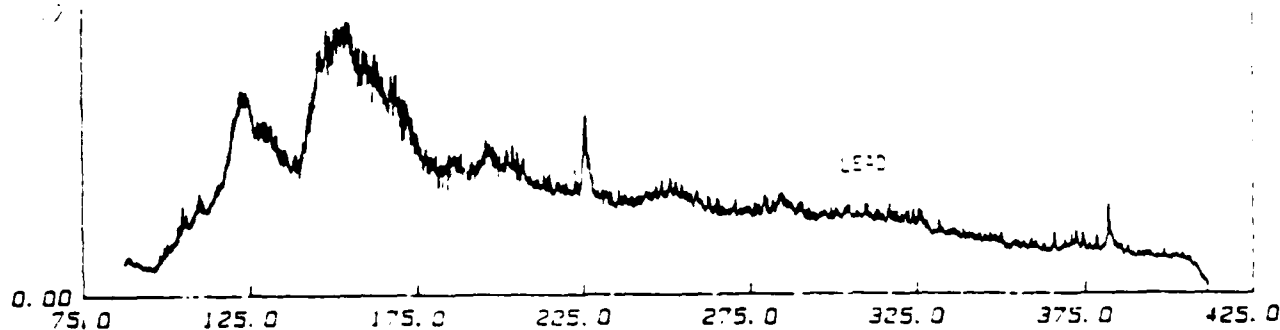
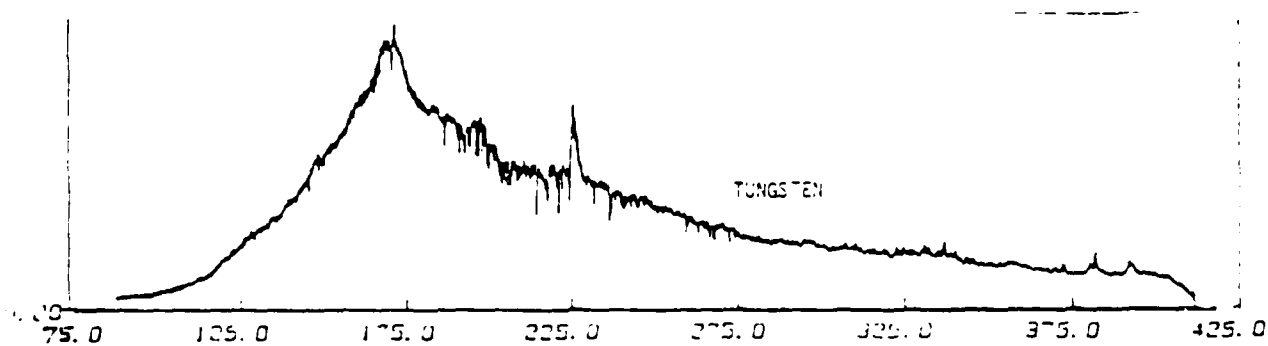
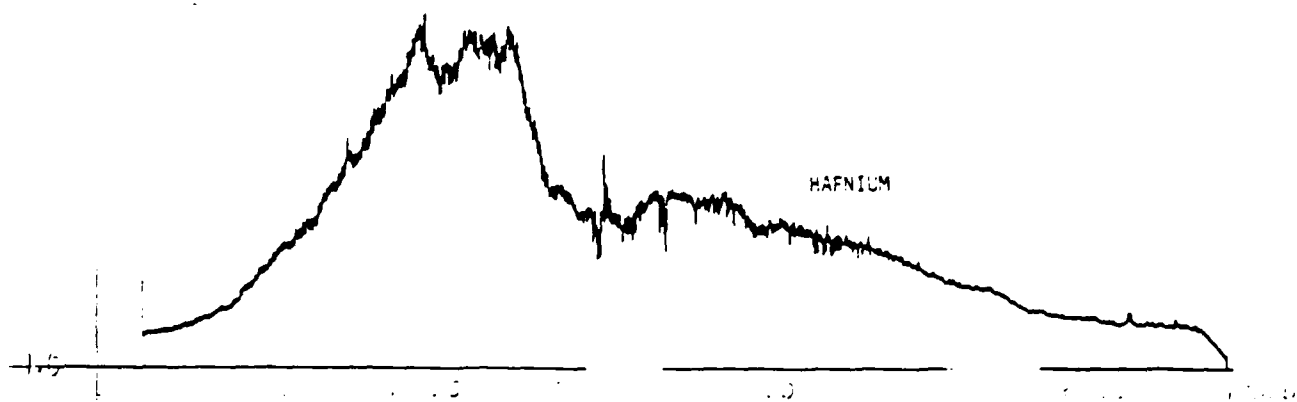
425.0

W. J. A.

1.1

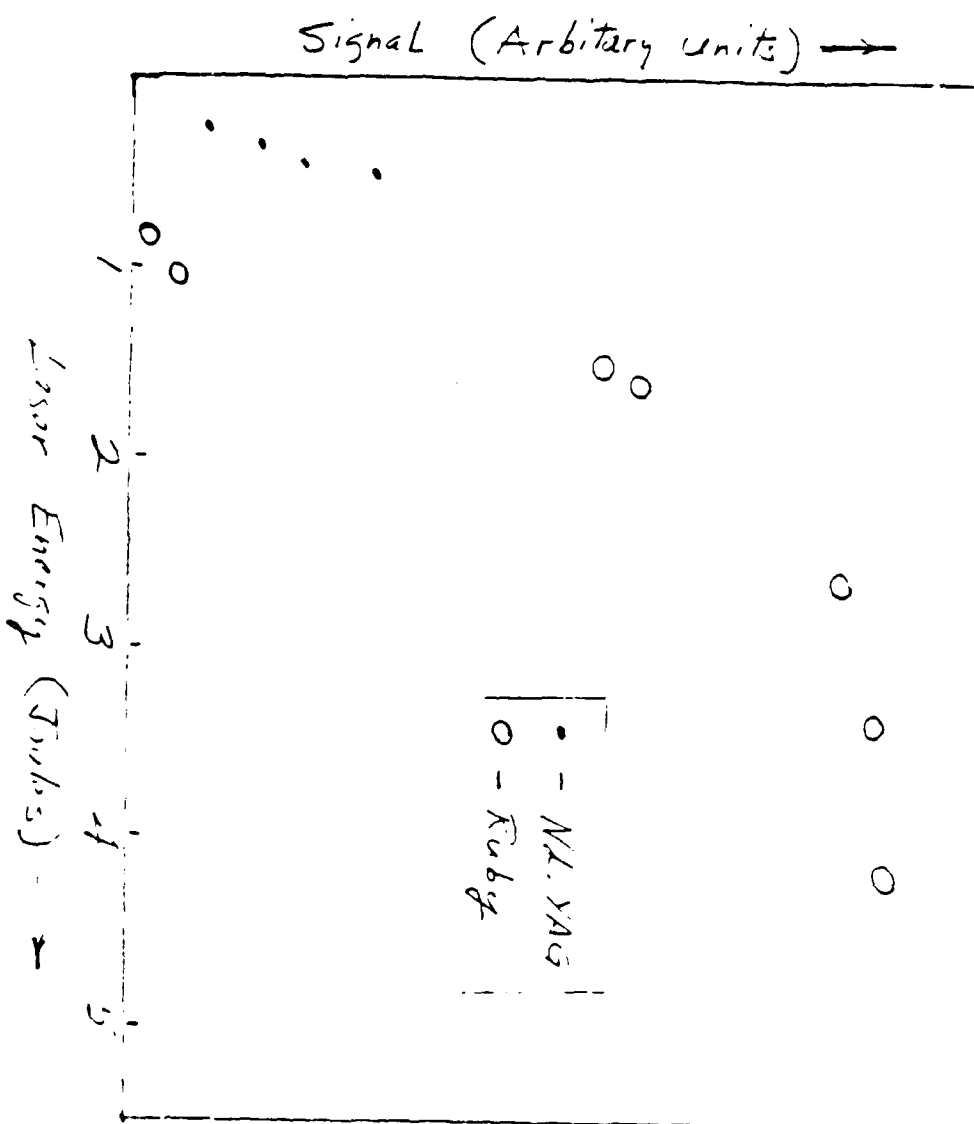
### Figure Captions

- Fig. 1. Diagram of target alignment.
- Fig. 2. Spectra from various target materials.
- Fig. 3. Dependence of signal on focus quality (Nd:YAG laser).
- Fig. 4. Dependence of signal on focus quality (Ruby laser).
- Fig. 5. Signal vs Laser Energy. Nd:YAG laser on Ytterbium target;  $\lambda = 20$  nm.
- Fig. 6. Signal vs Laser Energy. Nd:YAG and Ruby Lasers; tungsten target,  $\lambda =$ .
- Fig. 7. Ratio of signals from Hf target, for laser energies of 200 mJ and 500 mJ respectively.
- Fig. 8. Target damage for four target materials.



Copy available to DTIC does not  
permit fully legible reproduction

Fig 6



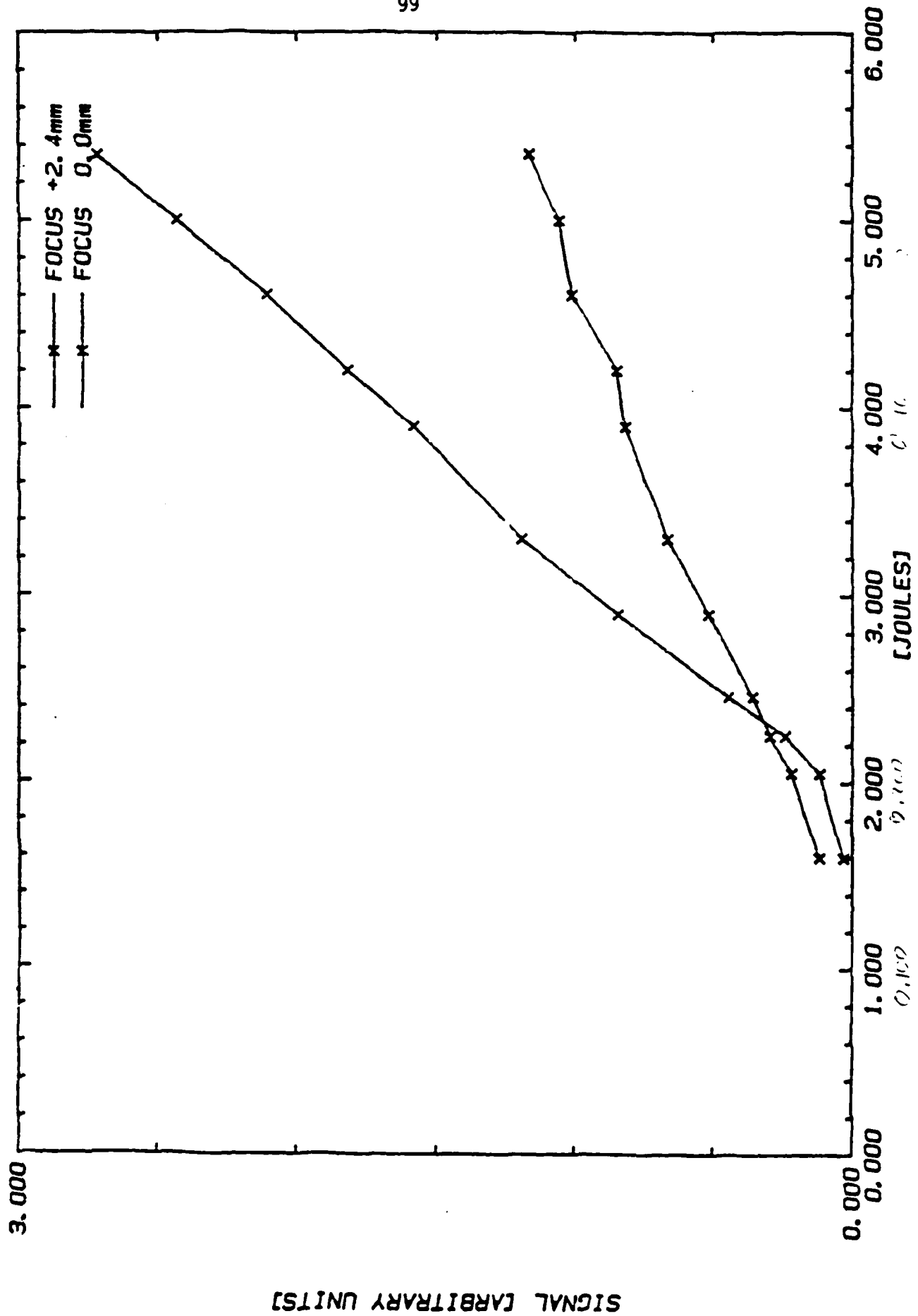
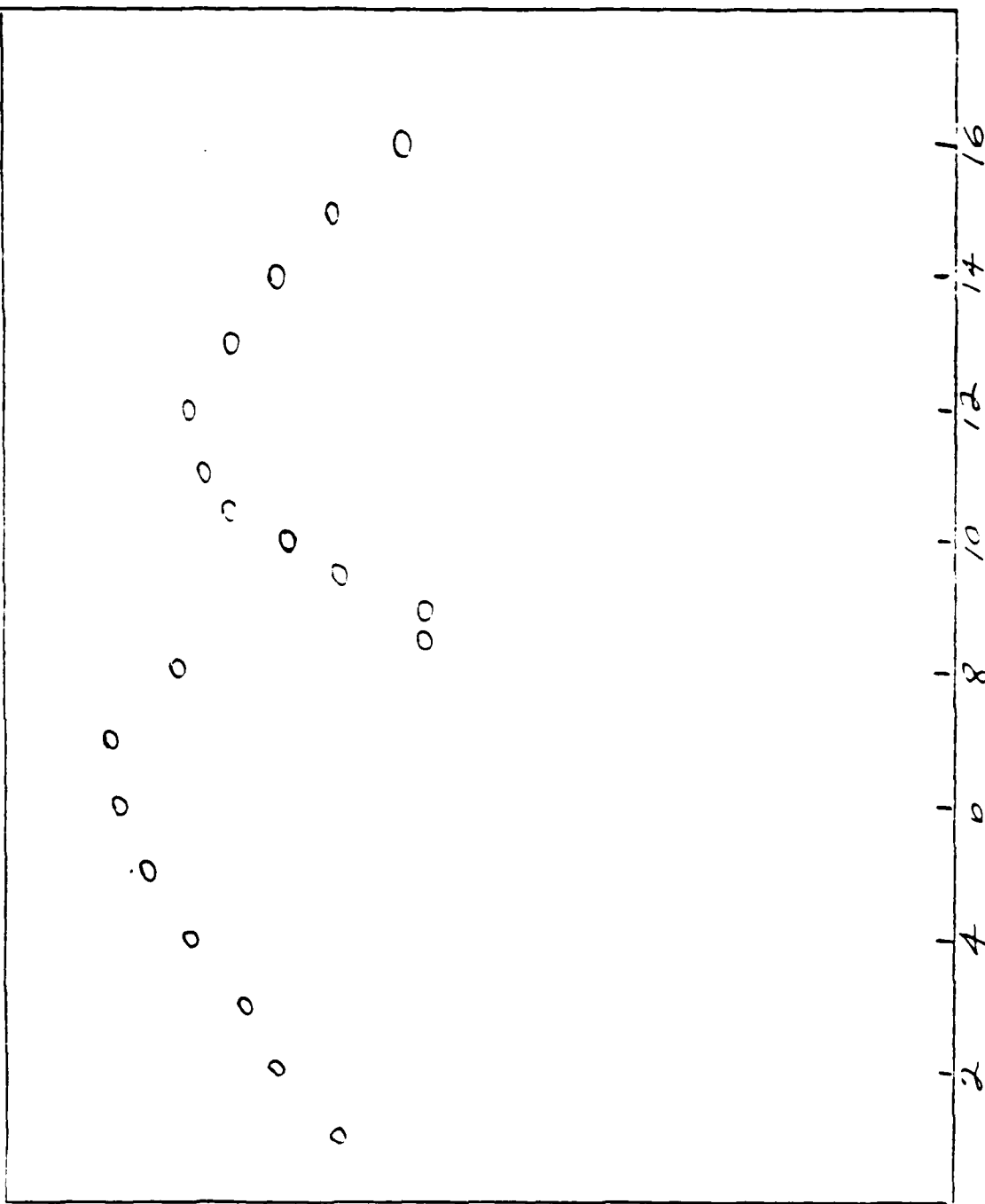


Fig. 5



Lens position (mm) ---

Fig. 3 Dependence of signal on lens position (mm)



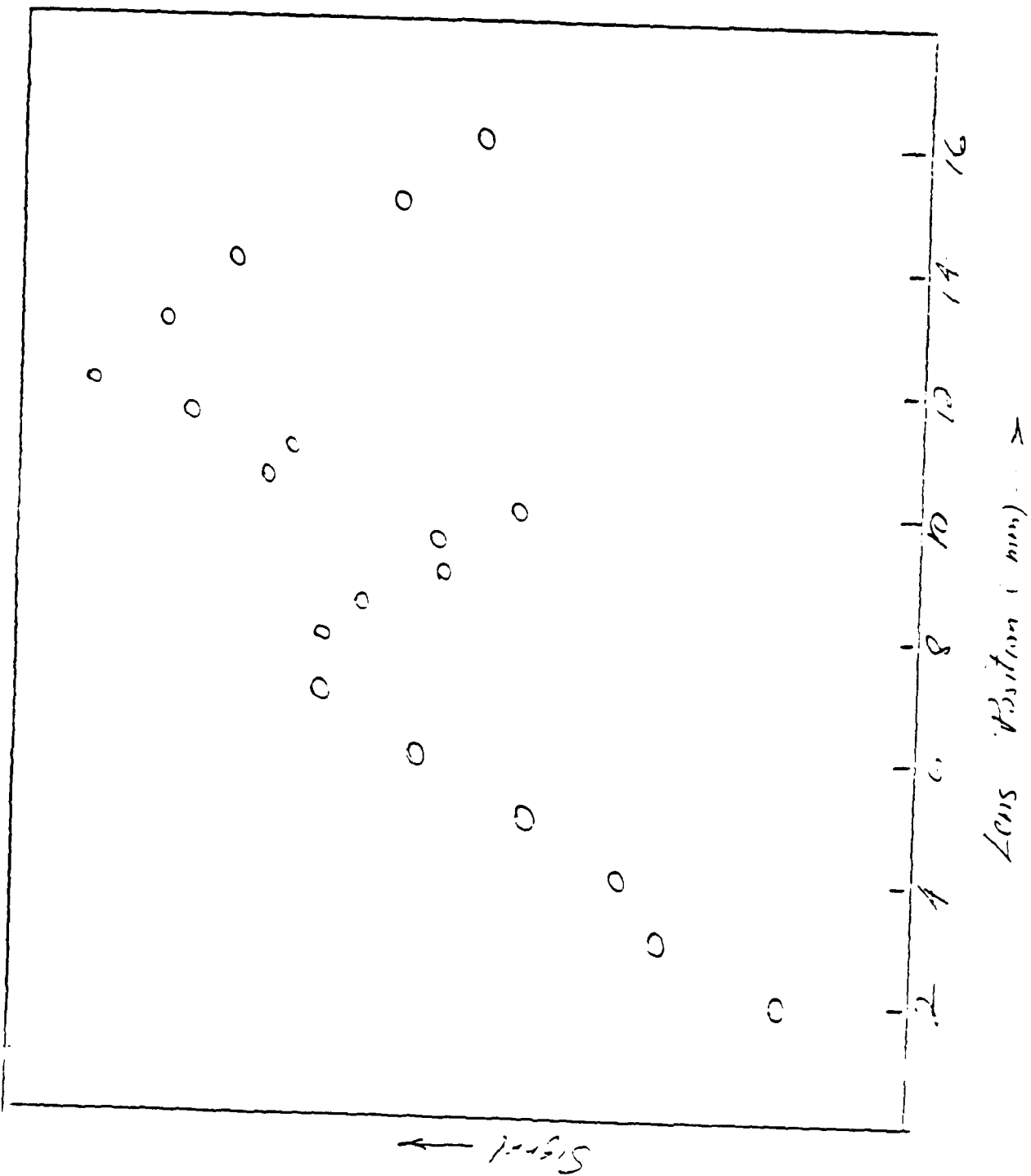


Fig 4. Dependence of signal on lens position (Ruby Laser)

Copy available to NRC does not  
 permit fully legible reproduction

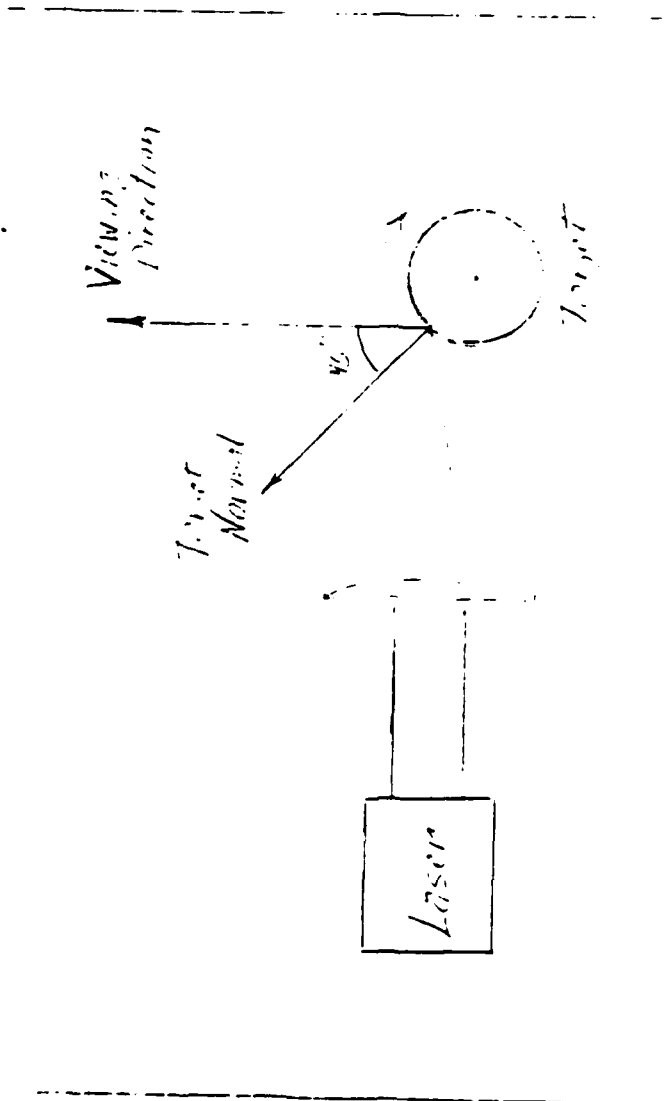


Fig. 1 Geometry of target illumination

END

6-87

Dtic